Authors' accepted manuscript
Article published in Reference Module in Materials Science and Materials Engineering, 2024.
The final published version available at https://doi.org/10.1016/B978-0-323-95486-0.00082-X

Recyclability of carbon nanomaterials-based conductive polymer composites

Emna Helal, Nicole R. Demarquette

Mechanical Engineering Department, École de Technologie Supérieure, Montréal, Canada

Abstract

Electrically conductive polymer composites (CPC) have a broad range of commercial applications including electronic packaging, capacitors, conductive adhesives and paints, membrane fuel cells, actuators, etc. CPC typically consist of an insulating polymer matrix and an electrically conductive filler which forms a continuous conductive network due to the percolation mechanism. Carbon-based nanomaterials, such as carbon black, carbon nanotubes, fullerenes as well as graphene and its derivatives, have been extensively studied as one of the most interesting classes of conductive fillers for CPCs, due to their unique geometries and combinations of functional attributes such as mechanical, thermal, optical and barrier properties.

With respect of the current green politics trends and the global transition toward a circular economy, an extensive research effort is dedicated to investigating the recyclability of plastics and related (nano)composites in order to make recommendations for best recycling and recovery practices for these materials. In this context, the recyclability of carbon nanomaterials-based CPC, as a growing class of polymer nanocomposites, seems to be a matter of a particular interest.

Keys words: conductive polymer composites, carbon nanomaterials, graphene, carbon nanotubes, carbon black, electrical conductivity, rheology, percolation threshold, recycling, additive manufacturing

Outline of the book chapter

Conclusion

Key points

- A review of the main carbon nanoparticles used in CPC.
- Detailed analysis of the key factors affecting electrical conductivity and electrical percolation threshold in CPC.
- Discussion on the evolution of conductive nanoparticle networks during melt processing and post-processing, along with recent advancements in using rheology to assess this evolution.
- In-depth discussion on recent progress in recycling carbon nanoparticle-based CPC.
- Insights on adopting additive manufacturing as a circular process for fabricating and recycling CPC.
- Examination of the benefits of carbon nanoparticles on the recyclability and durability of CPC.

Introduction

Conductive polymer composites (CPC), which consist of intrinsically insulating polymer matrices containing conductive fillers are used in a wide range of classical and emerging applications including energy storage and conversion [1, 2], sensors for various stimuli [3-14], electromagnetic interference shielding [3, 15-18], electrostatic discharge (ESD) apparatus, lightning strike protection, electro-optical devices as well as packaging and thermal interface materials for electronic devices [19-21]. CPC also present a significant light weighting advantage compared to metallic counterparts for example.

There are different classes of electrically conductive fillers that may added to intrinsically insulating polymer matrixes, including mainly: carbon-based fillers and metallic fillers [22, 23]. They can have micrometric or nanometric size and different geometries ranging from zero-dimensional to three-dimensional (spheres, tubes, rods, wires, platelets…). Their intrinsic electrical conductivities depend on their chemical natures as well as on their geometric attributes, among others. For instance, anisotropic fillers often feature different in-plane and through-plane conductivity values and can therefore result in CPCs with anisotropic electrical conductivity [24-26].

The most established carbon-based filler is carbon black (CB) which has found extensive applications in CPC for electrostatic dissipation (ESD) purposes, notably in power cables and rigid packaging, as well as for other purposes [9, 18, 27-35]. Graphite, too, has served as one of the oldest conductive fillers. More recently, the realm of carbon-based fillers has expanded progressively to encompass various carbon allotropes, including carbon nanotubes (CNT), graphene materials (such as few-layer graphene (FLG), graphene nanoplatelets (GnP), reduced graphene oxide (rGO)…) as well as other fullerenes and carbon fibers [1, 3, 5, 10, 35-40].

Metallic particles used in CPC include: nickel particles, silver particles [41], iron particles [42] and eutectic alloys [22, 23], among others. While metallic particles present higher intrinsic electrical conductivity values (as high as 10^6 $S.cm^{-1}$) and higher charging energy during tunneling

[19, 23, 43-45], some carbon-based fillers present the advantage of being more sustainable, easier to incorporate and process in polymer composites[46, 47]. Besides, they present less damaging effect on the mechanical flexibility of host polymer matrix. They present also other functional properties suitable to improve the performance and durability of prime and recycled polymers, such as: resistance to photodegradation [48-50], thermal stability [51], mechanical reinforcement [51, 52] and impermeability to water and oxygen [21]. This chapter will be limited to carbon nanomaterials-based CPCs.

Over the past decade, there has been extensive research into carbon nanomaterials-based CPCs. Experimental observations as well as analytical and numerical modeling have revealed that the electric conductivity of CPCs, along with several other functional properties, is influenced by several factors. These factors include the intrinsic electric conductivity, shape, size, specific surface area, volume fraction and spatial arrangement of the conductive particles within the polymer matrix [22, 30, 45, 53], as well as the chemical affinity and rheological properties of the polymer matrix [54, 55] Additionally, the processing and molding conditions play a crucial role [35]. It has been demonstrated, for instance, that, in melt compounding, factors such as mixing time and sequence, processing temperatures and post treatment (thermal annealing) significantly impact the final electrical conductivity of the resulting CPC [56-61].

Given the urgent necessity to embrace circular approaches facilitating the recycling of plastic products, including CPC, it becomes imperative to thoroughly contemplate the implications of all aforementioned factors in the design of recyclable CPC, aiming for enhanced performance and recyclability. To achieve this, it is essential to deepen our understanding and assessment of:

- the most critical factors affecting the electrical conductivity behavior of CPC, encompassing the intrinsic properties of the polymer matrix and conductive particles, along with processing and post treatment conditions
- the potential implications of reprocessing and recycling processes on the electrical conductivity and other functional properties of CPC.

The first part of this chapter delves into the critical factors influencing the formation of conductive networks and the electrical percolation threshold in CPC. The second part examines how the electro-rheological properties of CPC evolve during thermal annealing and shear deformation, as a tool to get insights about the sensitivity of conductive particle networks to thermomechanical stresses applied during melt processing or post-processing treatments which are also involved in mechanical recycling. The third part reviews recycling pathways for carbon nanomaterials-based CPC, primarily focusing on mechanical recycling methods. It explores the potential advantages of carbon nanomaterials in enhancing the durability, recyclability, and performance of recycled plastics, particularly in the context of closed-loop or extensive mechanical recycling.

I- Carbon nanomaterials-based conductive polymer composites

The purpose of this section is to provide a brief overview on 1) conductive polymer composites (CPC) as well as (2) main carbon-based nanomaterials currently used in CPC and their structures. Exhaustive reviews on these respective topics can be consulted elsewhere [5, 35, 62-65].

1-1) Conductive polymer composites

The majority of polymers are intrinsically electrical and thermal insulators. Electrical conductivity within initially insulating polymer matrices is achieved only when conductive particles are added to them at concentrations surpassing a certain threshold known as the **electrical percolation threshold (φ_c).** At this threshold, a continuous network of conductive particles is formed. φ_c is the critical reinforcement concentration at which the composite turns abruptly from insulator to conductor as conductive pathways are formed. Above the percolation threshold, the electrical conductivity exhibits a saturation effect, asymptotically approaching a maximum. Figure 1 illustrates a typical behavior of the formation and evolution of conductive filler network in CPC and the resulting transition from insulating to electrically conductive behavior [30, 45, 66, 67] in the vicinity of φ_c.

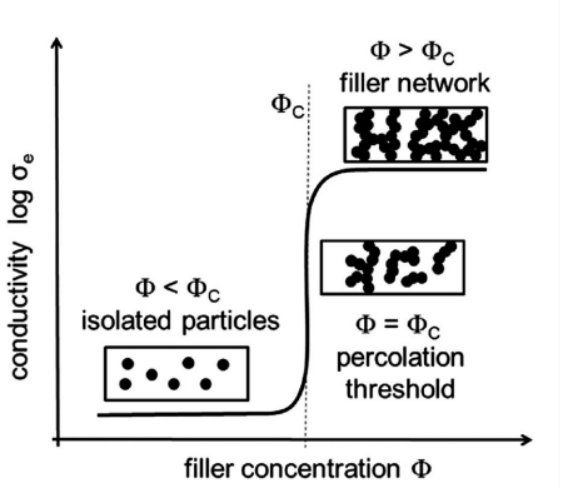

Figure 1: Schematic electrical percolation curve of conducting fillers in an insulating polymer matrix and evolution of conductive particles network in the different regions.
Reprinted with permission from reference [67]

The electrical conduction in CPC can occur by different mechanisms depending on the filler concentration. In general, at low filler concentrations, conduction is considered to occur via tunnelling between thin polymer layers between the fillers. As the filler loading increases, the filler particles come into contact with each other to form a conductive network, which facilitates charge transport within the composite. Near the percolation threshold, the conductivity increases sharply as a function of filler concentration which can be modeled by a power-law equation (1) [19, 63, 68].

$$\sigma_c = \sigma_0(\varphi - \varphi_c)^t \quad (1)$$

Where:
σ_0: proportionality constant related to the intrinsic conductivity of the filler
φ : filler volume fraction,
σ_f : filler conductivity,

σ_c : composite conductivity,
t: a scaling exponent, between 1.1 and 1.3 for 2D systems and between 1.6 and 2 for 3D systems [69, 70]
Besides the basic power-law model, several models have been developed to estimate the electrical conductivity of two-phase insulating polymer matrix/conductive filler composite materials by considering different factors and properties such as the shape, size and aspect ratio of the conductive nanoparticles as well as the thickness of the polymer/nanoparticle interphase region [30, 37, 71].

Achieving CPC with low percolation threshold concentration is highly desirable to maintain good mechanical flexibility, ease of processing, low density, and low cost. To achieve low φ_c, tailoring the dispersion and spatial arrangement of conductive fillers in the polymer matrix is critical. Specifically, the construction of a conductive network within an insulating polymer matrix requires a three-dimensional spatial distribution of fillers. However, the achievement of well individually dispersed fillers, as typically required for other properties, is not necessary [19]. On the contrary, the formation of secondary or loose agglomerates of individualized conductive nanoparticles facilitates the buildup of the conductive network at lower concentrations [66, 72]. Besides, the shape and size of conductive particles influence their spatial arrangement and consequently the percolation threshold concentration [37, 45, 73, 74]. The intrinsic electrical conductivity of the conductive filler has rather an effect on the maximum achieved conductivity of CPC [30]. The main types of carbon-based particles used in CPC and their characteristics s are discussed in the next section.

1-2) Carbon nanomaterials: review

The main types of carbon nanomaterials widely used in CPC are: carbon black (CB), carbon nanotubes (CNT) and graphene materials, such as graphene nanoplatelets (GnP) and few-layer graphene (FLG) [63, 75, 76]. The structures and relevant properties of CB, CNT and graphene are discussed in the following paragraphs. Extensive reviews on the topic can be found elsewhere [27, 34, 36, 77].

CB is the oldest member of the family of conductive carbon particles. It has been widely used in CPC due to its superior electrical conductivity and lower cost compared to other filler types such as CNT. However, the main disadvantage associated with the use of CB as conductive filler is the relatively high-volume fraction requirements, which lead, eventually, to the deterioration of mechanical properties and reduced processability of the CPC [30]. There are distinct types of CB depending on their production process. They differ in individual particle size, structure (aggregate size) as well as specific surface area [34, 78]. Common CB grades are typically obtained through thermal decomposition or incomplete combustion of carbonaceous gases [27]. In general, CB structures consist of individual particles of pseudospherical shapes arranged or fused into chain-like aggregated 3D structures, as seen in Figure 2(a). Each individual pseudospherical particle has a diameter ranging from 10 nm up to 500 nm [27]. Their internal structure is a form of para-crystalline carbon with a graphitic crystalline organization (but less ordered compared to graphite). It consists of layers of carbon that are partially oriented parallel to the surface and also around centers inside the particles, as illustrated in Figure 2(b) and Figure 2(c) [27]. Depending on the

number and arrangement of primary pseudospherical particles within the aggregated structure, on can refer to high structure CB or low structure CB. High structure carbon black has a high number of primary particles per aggregate, while low structure carbon black exhibits only a weak aggregation [79]. These aggregates themselves form loose agglomerates linked by Van der Waals interactions. The high structure CB are classified as specialty carbon black grades and typically feature high specific surface area. They are particularly used in applications requiring high electrical conductivity and therefore in CPCs. They are also referred to as conductive CB grades and allow to achieve robust conductive networks at lower concentrations compared to low structure CB grades, which can be used in other types of applications such as: UV resistance, mechanical reinforcement or color [32, 33, 38, 80]. The electrical conductivity of CB is in the range 10^1 to 10^3 S/m [45, 80].

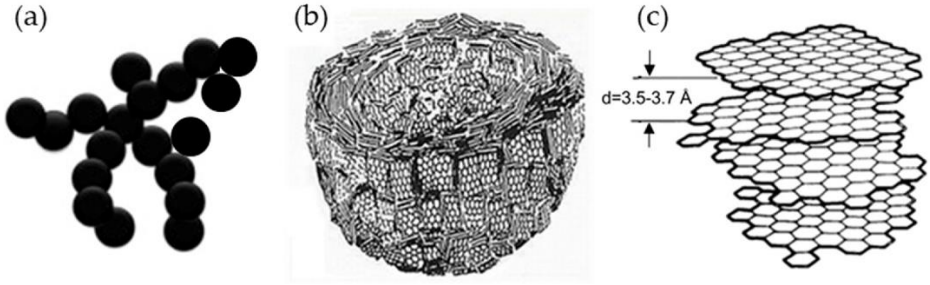

Figure 2: Structure of carbon black: (a) Carbon black aggregate, (b) aligned vortex layers of graphite domains, and (c) distance between carbon layers
Reprinted with permission from references [81, 82]

Figure 3 displays CNTs, graphene, and fullerenes. These are relatively recent nanoscale carbon allotropes that share the atomic arrangement of graphite, consisting of atom-thick layers of sp2-hybridized carbon atoms forming a honeycomb (hexagonal) lattice but with distinct geometries. Specifically, graphene and its derivatives are categorized as two-dimensional (2D) materials, having a platelet shape, and comprising one or more sp^2-bonded carbon atoms layers. CNTs, on the other hand, exhibit a tubular shape with one or more layers, making them one-dimensional (1D). Fullerenes are described as zero-dimensional (0D) due to their nanoscale spherical symmetry [36, 83].These carbon allotropes possess exceptional electrical, thermal, optical, mechanical, and other desirable properties, making them highly attractive as high-performance additives for polymer matrices. They impart significant multifunctional capabilities to these matrices [84]. In particular, the electrical conductivity of pure CNT and pure graphene can reach as high as 10^6 to 10^7 S/m and 10^8 S/m, respectively. These values are comparable to the two best metal conductors, silver and copper, which are equal to 6.30×10^7 and 5.96×10^7 S/m, respectively [45, 85].

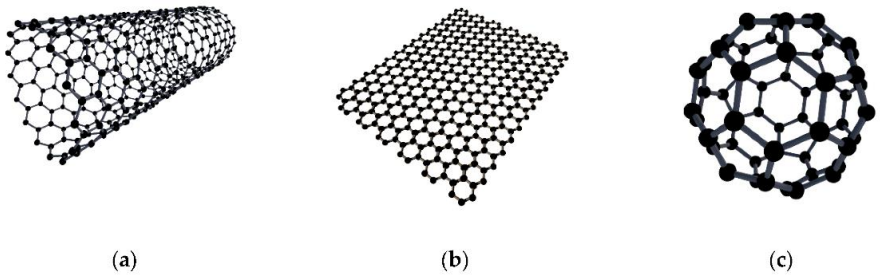

Figure 3: Atom structure of representative carbon-based nanomaterials: (a) carbon nanotubes, (b) graphene nanoplatelet, and (c) fullerene-C60
Reproduced from reference [84] under terms of the CC-BY license, Copyright 2020, MDPI

CNTs have extremely high aspect ratios (length to diameter) typically ranging from 100 to 1000, high specific surface areas in the range 100–1300 m^2/g and low densities in the range 1.3–2.0 g/cm^3 [83, 86]. Single walled carbon nanotubes (SWCNTs) comprise one single layer wrapped in the form of a cylinder with a diameter close to 1 nm. Multi walled carbon nanotubes (MWCNTs) consist of an array of concentric graphene cylinders with interlayer separations of 0.34 nm and typical diameters in the range 2–100 nm [83, 87]. MWCNTs are more widely used due to their relatively low cost, compared to SWCNTs.

As mentioned earlier, graphene consists of one or several planar sheets of sp^2 hybridised carbon atoms forming a honeycomb lattice. Graphene is the building block of graphite which is a three-dimensional (3D) crystal consisting of relatively weakly coupled graphene layers. It is also the parent form of CNT, fullerenes and the graphitic structures of carbon in general. By definition, the term graphene refers to a monolayer or single-layer graphene (SLG). But it is commonly used to refer to graphene materials in general. Multilayer graphene, also called few-layer graphene (FLG) or graphene nanoplatelet (GnP), contains up to 10 layers which are connected through weak van der Waals bonds. Their lateral dimensions range from approximately 100 nm to 100 μm according to ISO/TS 80004-13:2017. Further reduction in the dimensionality of graphene results in other forms known as graphene quantum dots and graphene nanoribbons. These materials exhibit finite bandgaps because of quantum confinement, making them attractive as next-generation semiconductors [88]. FLG or GnP are more widely used in different applications including CPC materials due to their availability at large-scale, ease of manufacture and low cost [89]. Besides, graphene has two main derivatives, namely graphene oxide (GO) and reduced-graphene oxide (rGO). GO could be obtained by oxidation of graphite and rGO could be synthesized by reduction of GO [90]. The specific surface area of graphene materials can reach up to 2630 m^2/g for single layer graphene and up to 1500 m^2/g for FLG [91]. The density of graphene is 2.26 g/cm^3 [86].

1-3) Main factors affection the electrical percolation threshold and electrical conductivity in CPC

Carbon nanomaterials-based CPCs have been extensively investigated in literature during the last decades. The purpose of this section is to provide an overview with focus on the factors affecting the electrical percolation threshold and electrical behavior of CPCs made from thermoplastic polymer matrices and through melt compounding processes, as they are more relevant in the

context of recycling. Comprehensive literature reviews regarding carbon nanomaterials-based CPCs can be consulted elsewhere. [5, 7, 14, 30, 35, 37, 67, 92].

Various polymers have been explored in conductive polymer composites (CPCs) depending on their intended application, ranging from commodity thermoplastics like polyethylene (PE), polypropylene (PP), and polystyrene (PS), to high performance thermoplastics like polyether ether ketone (PEEK) and polyimide (PI). For instance, in strain sensing applications, CPCs often employ thermoplastic elastomers such as thermoplastic polyurethane (TPU), styrene-ethylene-butadiene-styrene (SEBS), and ethylene vinyl acetate (EVA). As stated earlier, maintaining a low percolation threshold is crucial in CPC development to not only reduce costs but also to preserve the processability, flexibility, and other desirable properties of the polymer matrix. The electrical percolation threshold can vary widely, from extremely low values below 0.1 wt.% to higher values exceeding 10 wt.%. As an example. the percolation threshold tends to be higher in composites produced via melt compounding compared to those made through other less shear-intensive processes [45, 92-96]. In general, several factors influence the percolation threshold, including the nature and geometry of conductive nanoparticles, the rheological properties and polarity of the polymer matrix, the chemical affinity between the matrix and nanoparticles, as well as the specifics of the manufacturing processes and conditions [5, 18, 35, 54, 55, 57, 62, 66]. Each of these factors will be briefly discussed in the following paragraphs.

1-3-1) Effect of nanoparticle properties on the percolation threshold

With respect to the effect of nanoparticles geometry on the percolation threshold φc, it has been demonstrated that the percolation threshold is proportional to 1/l and to $1/l^2$ for disc shape (2D) fillers [97, 98] and cylinder shape fillers (1D) [99], respectively, where l is the effective length of the fillers. In contrast, for the conductive composites containing spherical fillers (0D), a roughly linear relationship exists between the percolation threshold and the filler diameter, $\varphi c \approx r$ [22, 30].

Alongside nanoparticles geometry, aspect ratio and specific surface area play important roles [64]. Ghislandi et al. [100] delved into the electrical percolation threshold and conductivity of PP nanocomposites incorporating CB, CNT, graphene, and graphite powders. They discovered that all four composite types reached maximum electrical conductivity at approximately 1.5 S/m, depicted in Figure 4(a). Notably, nanocomposites with MWCNTs and graphene exhibited the lowest percolation thresholds due to their higher aspect ratios and surface areas compared to CB and graphite powders. This facilitated the formation of conductive networks at significantly lower filler contents. In the same context, Pan et al. [101] explored how the aspect ratio of MWCNTs affects the electrical percolation threshold in PP nanocomposites containing MWCNTs with aspect ratios ranging from 51 to 167. Their findings showed a decrease in the percolation threshold with increasing aspect ratio. Furthermore, MWCNTs with larger aspect ratios could create denser conductive networks, resulting in higher electrical conductivity for the composites (Figure 4(b)). Similarly, Karásek et al. [53] examined the impact of CB's specific surface area on the electrical percolation threshold in styrene-butadiene rubber (SBR)/CB composites and observed a decreasing percolation threshold trend with increasing CB specific surface area.

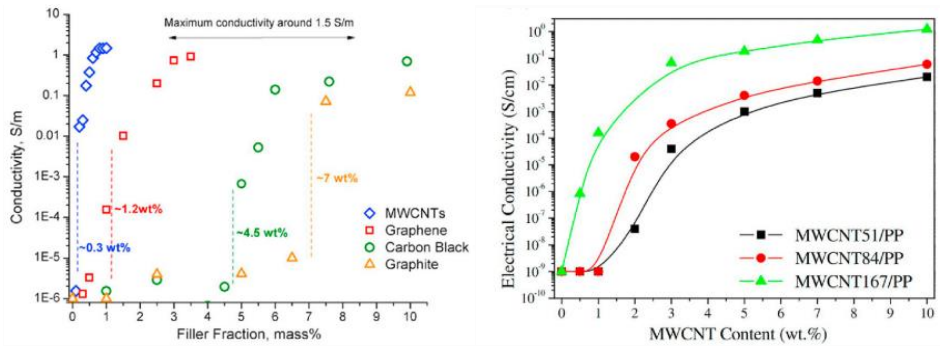

(a) **(b)**

Figure 4: (a) Electrical conductivity of polypropylene (PP) composites containing different carbon fillers (MWCNT, graphene, graphite and CB) as function of filler concentration (reprinted with permission from reference [100]), (b) Electrical conductivity of PP/MWCNT nanocomposites with different aspect ratio as function of filler content (reprinted with permission from reference [101])

1-3-2) Effect of polymer properties on the percolation threshold

Each polymer is having different characteristics that can affect the electrical percolation threshold and electrical conductivity of CPC materials such as: viscosity, crystallinity, polarity, inherent conductivity, and affinity with the selected conductive nanoparticles [30, 54, 55, 64, 102, 103]. In particular, the viscosity of the polymer matrix plays a key role on the electrical percolation threshold. Socher et al.[55] investigated the effect of polymer matrix viscosity on the electrical percolation threshold of five different thermoplastics incorporating MWCNTs. The chosen polymers, namely polyamide 12 (PA12), polybutylene terephthalate (PBT), polycarbonate (PC), polyetheretherketone (PEEK) and low-density polyethylene (LDPE), feature also different characteristics: (polar, non polar, amorphous or crystalline). The authors observed significant differences in the electrical percolation thresholds of CPCs made with the same polymer matrix but with different viscosity grades. An example of this behavior is illustrated in Figure 5, for PA12. In a general trend, the lowest percolation thresholds were observed in the composites based on the low viscosity matrices. A similar behavior has been reported by Helal et al. [54] for thermoplastic/graphene composites. This behavior was attributed to the presence of more secondary agglomerates of conductive particles in the low viscosity materials, which are necessary for the formation of conductive networks, as well as to the restricted mobility of the conductive nanoparticles in high viscosity matrices.

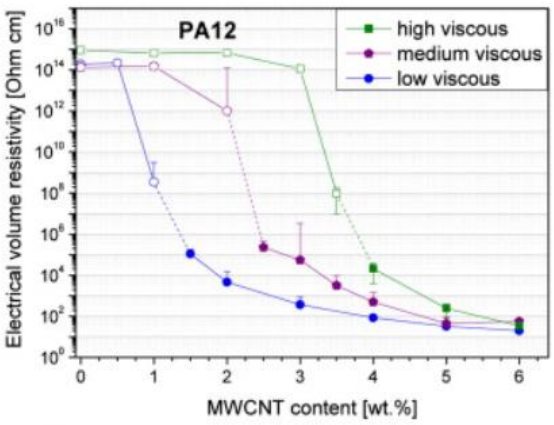

Figure 5: Electrical conductivity of polyamide 12 (PA12)/MWCNT nanocomposites as function of MWCNT content in composites based on PA12 matrices with different viscosities
Reprinted with permission from reference [55]

The impact of polymer polarity on the electrical percolation threshold has yielded conflicting findings in the literature. On one hand, certain studies suggest that the presence of polar groups in a polymer matrix enhances its affinity with carbon-based fillers, thus aiding in the formation of conductive networks [104]. Conversely, other research indicates that highly polar groups, like amide groups in polyamide, can encapsulate carbon black nanoparticles, thereby restricting the interphase region and impeding the formation of conductive networks [30].

Opposite effects have been also reported regarding the effect of polymer matrix crystallinity on the electrical percolation threshold, also depending on the polymer/carbon nanomaterial composite system. Al-Saleh [103] studied the electrical percolation behaviors of CB, CNT and GnP in an amorphous polymer and a semi-crystalline polymer, respectively PS and PP, of similar viscosities. His findings suggest two possible effects of crystallinity: 1) a decrease of conductivity and an increase of the percolation threshold attributed to partial wrapping or growth of a crystalline layer on the surface of conductive nanofillers during cooling from the molten polymer, 2) no effect on the electrical conductivity if crystal growth takes place in spaces between nanoparticles network without affecting their distribution. A similar trend has been observed in other studies [105]. On the other hand, increase of electrical conductivity and decrease of the electrical percolation threshold with crystallinity have been demonstrated in certain polymer/carbon nanoparticle systems and attributed to the volume exclusion effect, i.e., conductive networks are expelled from the crystalline region growing during cooling from the melt and form denser conductive networks exclusively in the amorphous phase of the polymer [93, 106]. The volume exclusion effect will be discussed further in a following section dealing with the main approaches to reduce the electrical percolation threshold in CPCs.

1-3-3) Effect of the manufacturing processes and conditions

Due to differences in interfacial energy between particles and the polymer matrix, particles and their aggregates tend to clump together or flocculate during further processing or post-processing. This results in filled conductive polymer composites being seen as thermodynamically non-

equilibrium systems. In these systems, the formation of conductive particle networks and the percolation threshold depend on factors like temperature, time, and thermo-mechanical stresses encountered during melt processing and post-processing. Changes in these factors lead to variations in electrical conductivity and percolation threshold, which are caused by particle diffusion, migration, and the subsequent evolution of conductive networks. This phenomenon is referred to as dynamic percolation threshold [39, 53, 59, 107, 108]. Consequently, careful consideration of processing parameters is essential in both fabricating CPC and mechanically recycling them through melt compounding processes. In the following, a brief review of the main processing parameters that affect the electrical percolation behavior is presented. The recycling of CPC will be discussed in the next section of this chapter.

Shear and extensional deformations involved in various melt processing methods such as extrusion and injection molding can lead to different thermo-mechanical stresses and direct effects on conductive particle networks of CPC materials [14]. Kuester et al. [57] studied the electrical behavior of styrene ethylene butadiene styrene (SEBS)/CNT nanocomposites prepared by sheet extrusion and compression molding, respectively. The authors found that the electrical percolation threshold of the SEBS/CNT nanocomposites produced by sheet extrusion is lower than those fabricated by compression molding. At 2 wt.% CNT, the difference in electrical conductivity between both types of composites was around 6 orders of magnitude. This behavior has been attributed to the difference in CNT distribution in both types of materials: random distribution in composites prepared by compression molding vs. aligned distribution in the composites prepared by tape extrusion due to high shear forces applied in the extrusion direction. The CNT alignment in the latter case induced an anisotropic electrical conductivity, with the lowest value being perpendicular to the CNT alignment direction selected for conductivity measurements.

Another example of control of conductive networks via shear deformations has been reported by Tjong et al. [109]. They evaluated the effect of different shear rates applied during melt mixing on the electrical behavior of PP/MWCNT nanocomposites. They found that the nanocomposites prepared at high shear rates exhibited much lower percolation threshold than those fabricated at low shear rates (0.22 vol.% vs. 1.31 vol.%). This behavior has been attributed to the better dispersion and more uniform distribution of MWCNT achieved in PP under intensive shearing compared to clusters of large agglomerations observed in the low shear rates nanocomposites, as illustrated in Figure 6(a).

In addition to the type and intensity of thermo-mechanical stresses applied during melt mixing, the mixing time plays an important role on the formation of conductive particle networks in CPC. Kou et al. [56] investigated the effect of mixing times ranging from 1 to 20 mins on the electrical conductivity of polylactide (PLA)/poly(ethylene-co-vinyl acetate (EVA) co-continuous blends containing 0.5 wt.% GnP. They found that the electrical conductivity increases with increasing mixing time up to 5 mins then starts decreasing at 10 mins. Then, a significant decrease of conductivity of 3 orders of magnitude was observed for the composite obtained after 20 minutes of mixing, as illustrated in Figure 6(b). They explained this trend by the fact the GnP particles tend to migrate from the PLA phase, to which they have less chemical affinity and form a conductive network at the interface PLA/EVA. The increasing mixing time up to 10 minutes enables more

GnP particles to migrate to the interface and to achieve good interfacial coverage. However, at higher mixing times, the GnP particles kinetically trapped at the interface continue their migration to the more thermodynamically favorable EVA phase. This process is illustrated in Figure 7. Besides, an isothermal annealing up 1 hour of the different samples induced a slight increase of the electrical conductivity indicating that thermal energy alone doesn't induce a significant change in the conductive networks in this nanocomposites system (less than 1 order of magnitude). It is worth noting that in this study, the PLA/EVA/GnP blend nanocomposites were prepared by a two-steps mixing method, where GnP were first premixed with the less thermodynamically favorable PLA phase, to promote their migration to the blend interface during melt mixing. More details about this topic will be discussed in the next section dealing with approaches to reduce the electrical percolation threshold in CPCs.

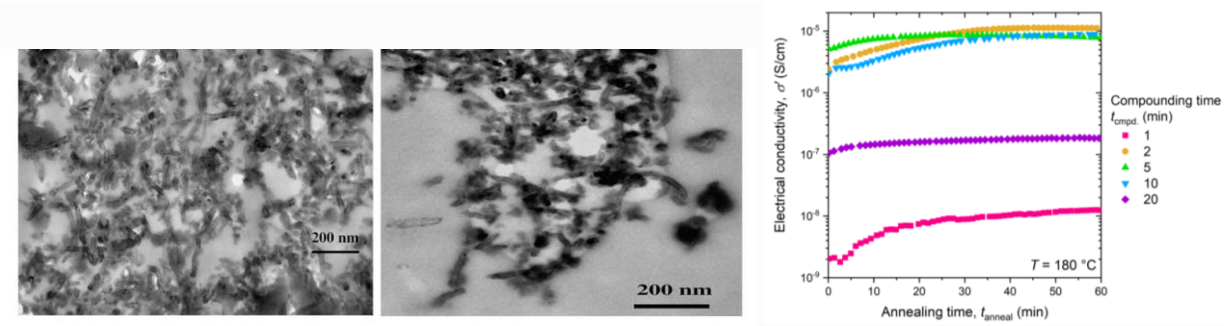

(a) (b)

Figure 6: (a) TEM images of PP/MWCNT nanocomposites processed, respectively, at high and low shear rates (reprinted with permission from reference [109]), (b) effect of melt compounding time on the electrical conductivity of co-continuous PLA/EVA blends containing 0.5 wt.% GnP. The electrical conductivity is measured continuously during an isothermal annealing at 180 °C, using a dielectric rheology cell (reprinted with permission from [56])

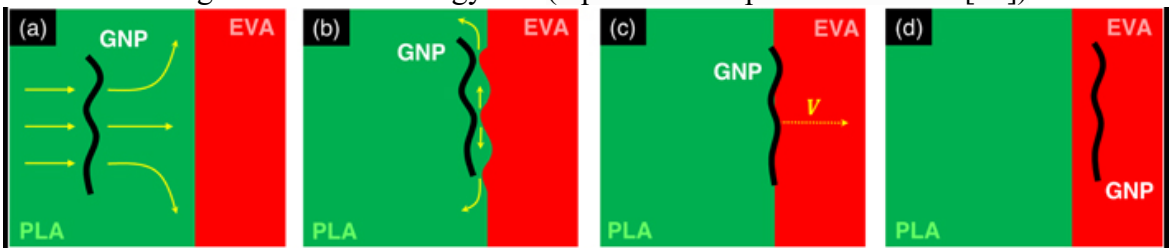

Figure 7: Illustration of GnP migration steps from PLA to EVA in PLA/EVA blend during melt mixing: (a) bulk migration far from the interface, due to convection by the compounding flow with the background PLA matrix, (b) film drainage of the departing phase at the interface, induced by the attractive interactions between GnP and EVA, (c) the displacement of the three-phase contact line at the filler surface, and (d) eventual particle migration across the interface into the preferred EVA phase
Reprinted with permission from reference [56]

Changes in time and temperature conditions in less shear-intensive processes such as compression molding could also have a significant impact on the electrical conductivity and percolation threshold of some CPC materials [5]. In this context, we studied the electrical conductivity of PP/CB and PP/GnP nanocomposites hot pressed at different times and temperatures. The loadings

of GnP in the studied nanocomposites were equal to 20 and 25 wt.% while those of CB were equal to 5, 7 and 10 wt.%. The results, presented in Figure 8, show that the electrical conductivity of both PP/GnP and PP/CB increases with increasing time and temperature by up to 2 orders of magnitude at selected concentrations. This behavior is most likely attributed to the formation of more secondary agglomerates and strengthening of the conductive networks, due to facilitated diffusion/flocculation of conductive particles at increased temperature and/or time [58].

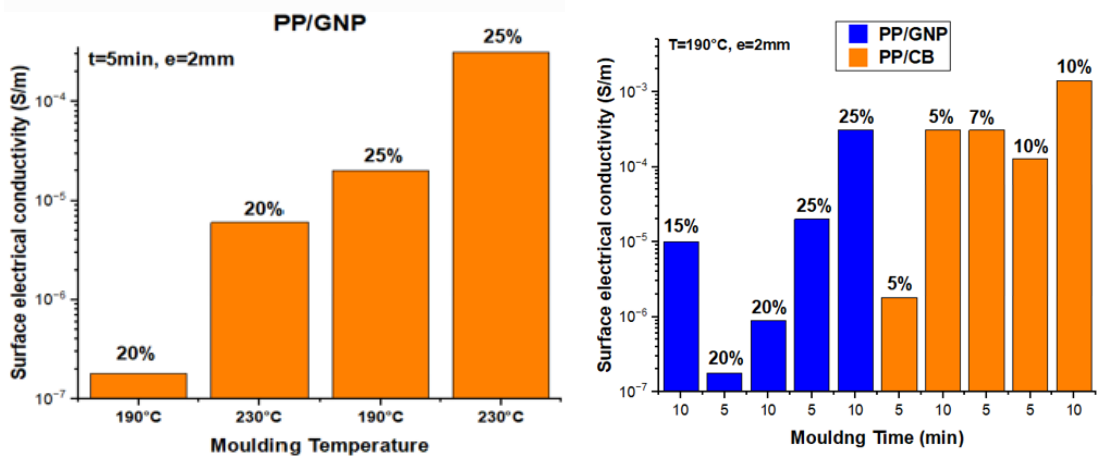

Figure 8: Effect of compression molding conditions, (a) varied temperatures at a fixed press time of 5 mins and (b) varied time at a fixed temperature of 190 °C (samples thickness e = 2mm), on the electrical conductivity of PP nanocomposites with different loadings of CB and GnP (Courtesy of MSc student Omayma Belgacem)

In the same context, Zhang et al. [59] investigated the electrical conductivity/resistivity behavior of high-density polyethylene (HDPE)/poly(methyl methacrylate) (PMMA)/carbon fiber (CF) conductive composites, hot-pressed at different temperatures for varied periods of time. They measured the room temperature electrical resistivity at each time and temperature molding condition and plotted the resistivity as function of molding time for each studied temperature. The results are summarized in Figure 9. It can be observed that at a given temperature, the electrical resistivity decreases slightly with increasing pressing time at the early stage, and then decreases rapidly at a critical time, indicating the formation of a conductive network in the composite. This phenomenon was attributed to the rearrangement of short carbon fibers in the filler-rich HDPE phase during the compression molding process. Consequently, the critical time, at which the first conductive network is constructed throughout the composite, is referred to as the percolation time. This characteristic time decreases with increasing pressing temperature, which can be correlated with the reduction of the viscosity of the matrix at higher temperatures.

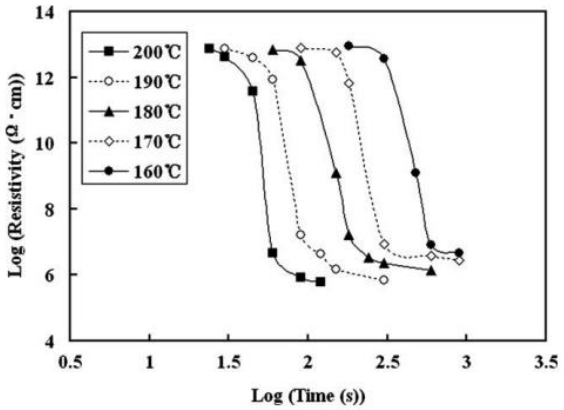

Figure 9: time dependence of room temperature electrical resistivity of HDPE/PMMA/CF blend nanocomposites hot pressed at different temperatures ranging from 160 °C to 200 °C and for a varied period of time
Reprinted with permission from reference [59]

1-3-4) Approaches to reduce percolation threshold in CPC

Several approaches have been investigated to reduce the electrical percolation threshold in carbon nanomaterials-based CPCs [14, 45], essentially using hybrid fillers [16, 110], selective localization of carbon fillers in polymer blends [19, 110-115] or the achievement of segregated conductive structures or networks [19, 107].

In particular, the use of hybrid conductive fillers in CPCs is an effective approach which consists of combining different types of fillers with different geometries for instance, to facilitate interparticle bridging and formation of interconnected conducting networks, and to enhance processing and/or other functional properties synergistically [19, 116]. For example, Maiti et al. [117] and Kuester et al.[16] showed that the electrical and rheological percolation threshold could be reduced if a combination of carbon based nanofillers would be used instead of a single type of carbon based nanofillers. Kuester et al. [16] showed that hybrid nanocomposites containing simultaneously MWCNT and GnP nanofillers featured synergetic effects in electrical conductivity and electromagnetic shielding effectiveness when compared to nanocomposites containing similar concentrations of single nanofillers. Maiti et al. [117] had explained this behavior through a bridging effect between the aromatic rings present in the polymer matrix, polystyrene (PS) in this case, and the different carbon additives as shown in Figure 10.

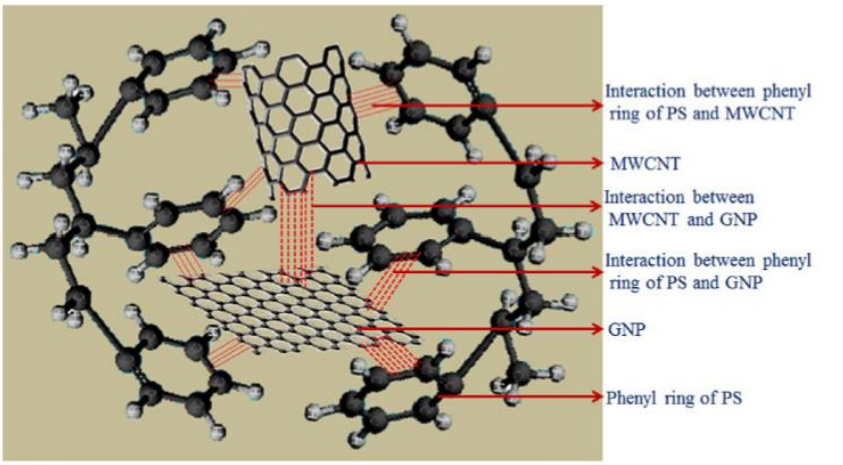

Figure 10: Schematic representation for π-π interactions between GnP, MWCNT, and PS in hybrid nanocomposites of PS/MWCNT/GnP
Reprinted with permission from reference [117]

Another approach widely used to reduce the electrical percolation threshold is based on the use of immiscible polymer blends as matrices, in particular blends with co-continuous morphologies. This approach involves the selective localisation of fillers, exclusively, in certain phases of polymer blends. In this case, percolated conductive networks form within one continuous phase of the polymer blend, leading to a reduction of the percolation threshold. The selective localisation of the conductive fillers at the interfaces of co-continuous polymer blends can reduce even further the amount of filler required to form a percolated network [58, 60, 61, 93, 114, 116, 118]. Figure 11, by Nofar et al. [119], visually represents the concept behind this selective localization approach. In this context, discussions often revolve around double percolation and triple percolation. Specifically, double percolation refers to the selective localization and percolation within a polymer phase that forms continuous channels and is itself percolated throughout the polymer blend [116]. On the other hand, triple percolation involves the formation of conductive networks in a continuous polymer phase of a ternary blend, which is selectively positioned at the interface of the other two phases forming the polymer blend [28].

The selective localization of third phase, in the present context conductive nanofillers in a particular phase or at the interface of a polymer blend depends on thermodynamic factors related to the affinity between the third phase and the polymers of the blend and kinetic factors involving the compounding strategy, in addition to factors related to third phase geometry and rheological properties of the polymer phases, among others [120] .

Practically, for a specific nanoparticle/polymer blend system, the thermodynamically preferred localization of the nanoparticles in the blend is predicted by evaluating the wetting coefficient using Young's equation, based on interfacial tensions between the different components of the system: the nanoparticle and each of the polymer phases [121].

$$w_a = \frac{\gamma_{Nanoparticle-A} - \gamma_{Nanoparticle-B}}{\gamma_{A-B}} \quad (2)$$

Where:

γ_{X-Y} represents the interfacial tension between component X and component Y

If ωa > 1, the fillers are preferentially located in polymer B; if ωa < −1, the fillers are preferentially located in polymer A and if −1 < ωa < 1, the fillers are expected to locate at the blend interface

The interfacial tension between 2 components can be calculated by the Harmonic-mean equation or the Geometric-mean equation, knowing the surface tension of each component. Surface tensions (or surface energies) of different polymer types can be found in literature or can be measured, using the pendant drop method for instance [122]. It is worth noting however that surface tension values of nanoparticles are difficult to determine experimentally and those reported in the literature may present significant variation depending on the specifications of the studied nanoparticle, particularly its surface chemistry. This is one limitation of this prediction method. However, it remains widely used to get insights, when considering a selective localization approach. More details regarding the thermodynamic prediction of nanoparticles localization as well as reported surface tension values for some carbon-based nanomaterials can be found elsewhere [111] .
Considering the thermodynamically preferred localization of nanoparticles in a specific blend system, kinetic arrest of nanoparticles at the blend's interface can be achieved by tailoring: compounding strategy (mixing sequence, time, shear rate), polymer's viscosities as well as nanoparticles geometry and surface chemistry. All these factors control directly blend's morphologies as well as the diffusion and migration of nanoparticles during melt mixing and processing [56, 118, 123]. One of the frequently reported strategies is to adopt a two melt mixing steps where the nanoparticles are initially premixed with the less thermodynamically favorable polymer phase, to promote their migration towards the thermodynamically preferred polymer phase, added in a second mixing step. Subsequently, kinetic arrest of the migrating particles at the blend interface is achieved by controlling mixing time and shear rate [56, 111, 113, 124].

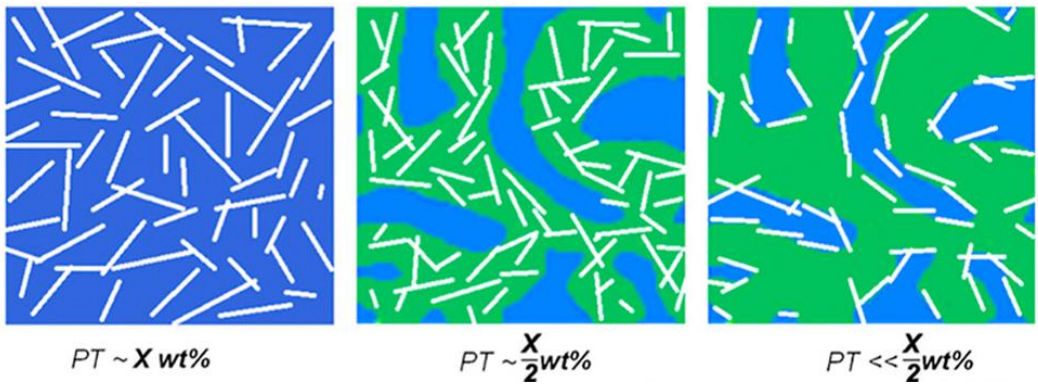

Figure 11: Illustration of the effect of selective particles localization on the reduction of the percolation threshold (referred to as PT): random distribution in single phase polymer vs. selective localization in 1 phase of a polymer blend vs. localization at the interface
Adapted with permission from reference [119]

A third approach utilising a segregated structure has proven to be effective in producing polymer composites with high electrical and/or thermal conductivities and low percolation thresholds [19, 93, 125, 126]. This approach has proven especially efficient for materials that are semi-crystalline, through the application of a thermal annealing. More precisely, by choosing a proper annealing temperature which favors greatly the growth of spherulites (isothermal crystallization), it is possible to push the conductive nanoparticles towards their borders, resulting in a volume exclusion effect, from the crystalline to the amorphous regions, and therefore reduction of the electrical percolation threshold [93, 125]. Figure 12 illustrates the principle of this approach. For instance, this technique was used by Kazemi et al.[126] to reduce by nearly 50% the percolation threshold concentration of PP/MWCNT nanocomposites, from 0.86 wt% to 0.45 wt%.
However, it's crucial to note that the exclusion effect is closely tied to the selected isothermal annealing temperature and pressure. The chosen annealing conditions must effectively suppress the heterogeneous nucleation ability of carbon nanofillers to achieve the desired exclusion effect. Otherwise, promoting heterogeneous crystal nucleation during annealing may lead to an undesired outcome, such as wrapping the CNTs with an insulating layer of crystalline polymer and increasing contact resistance [126].

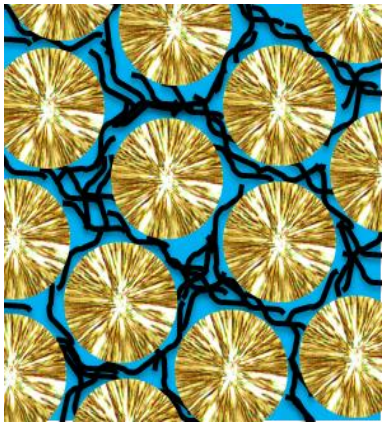

Figure 12: CNT (in black) pushed away from the growing spherulites (in gold) and selectively located in the amorphous polymer phase (in blue) after thermal annealing (Courtesy of Dr. Daria Strugova)

Segregated structures can be created by compression moulding a mixture of polymer granules coated with conductive fillers through a mechanical mixing process, such as dry mixing. The mixing of the polymer and carbon fillers at the solid-state leads to the formation of segregated networks of conductive fillers during compression molding, unlike melt compounding or solution mixing which typically induce more homogeneous distribution of conductive fillers and higher percolation threshold, as illustrated in Figure 13. Segregated conductive networks typically lead to CPCs with ultra-low φ_c, high electrical conductivity and high EMI shielding properties [19, 63, 75, 127]. For example, Jia et al. [127] compared the electrical conductivity and EMI shielding performance of PE/CNT nanocomposites with segregated structures (s-CNT/PE) and randomly distributed structures (r-CNT/PE). s-CNT/PE were achieved through mechanical mixing of crosslinked PE granules with CNTs followed by compression molding while r-CNT/PE were

prepared solution blending followed by compression molding. The percolation threshold values were evaluated at to 0.013 and 0.310 vol% for s-CNT/PE and r-CNT/PE, respectively. Besides, at 0.8 wt.% CNTs, the s-CNT/PE composite exhibited an electrical conductivity equal to 0.89 S m^{-1}, more than two orders of magnitude higher than that of r-CNT/PE nanocomposites.

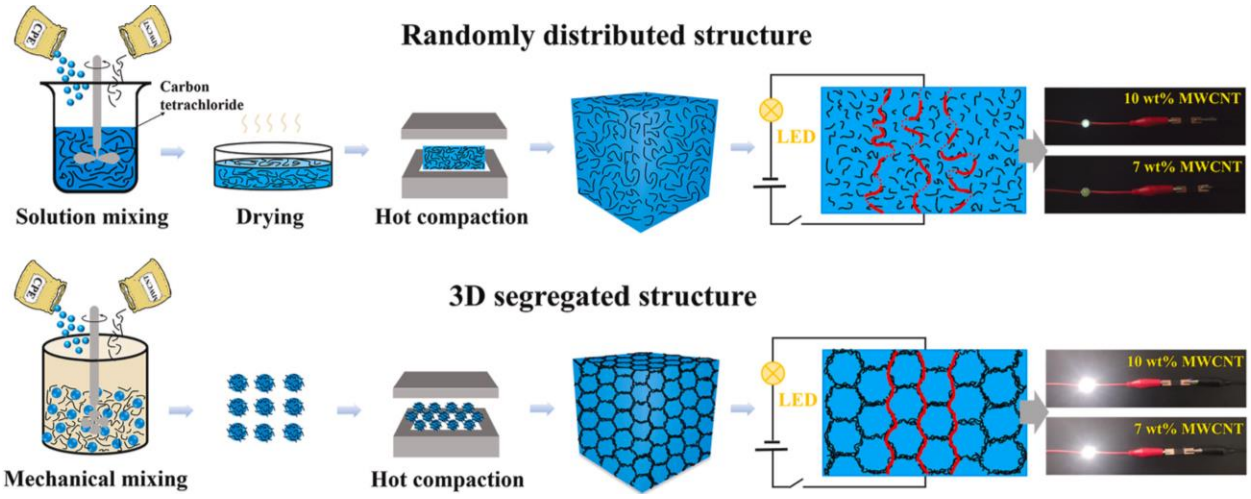

Figure 13: schematic diagram for the preparation of CPE/MWCNT composites of randomly distributed structure and 3D segregated structure respectively by solution mixing and mechanical mixing
Reprinted with permission from reference [75]

II- Rheology as a tool to characterize conductive nanoparticles network and its evolution during processing and recycling

As discussed in the previous section, nanoparticles need to be adequately spatially distributed, and the composite must exhibit appropriate morphology to conduct electricity. After ensuring satisfactory design of CPC, the composites might undergo additional processing involving shear and extensional flows, especially during recycling. However, even if an initially well-designed polymeric device conducts electricity, grinding it down and reprocessing could alter its morphology due to flow-induced changes in the composite, potentially leading to a loss of conductivity. Hence, it is crucial to grasp how the morphology and conductive particles networks of CPC will evolve when subjected to flows.

Fortunately, the morphology of multiphase polymer systems and their evolution under controlled flow can be studied through the analysis of their rheological behavior. Rheological characterization in the linear viscoelastic regime (LVE) allows for the quantification of morphology by fitting constitutive equation to it, while in the nonlinear viscoelastic regime (NLVE), it provides information upon its evolution during processing [128]. Below, the principles of these analyses will be presented. Specifically, we will show how rheology can be used to characterize the morphology of conductive composites and will demonstrate how the morphology of conductive composites evolves during annealing and how it is possible to integrate rheology with electrical

measurements to comprehend the changes in morphology and electrical conductivity of conductive composites during processing and recycling.

2-1) Concept of rheological percolation

Molten polymers exhibit a viscoelastic rheological behavior. When subjected to stress, they initially deform and continue deforming over time. Conversely, subjecting a polymer to constant deformation results in instant stress, which gradually decays over time. This behavior is known as stress relaxation. In cases of small and slow deformations, the resultant stress exhibits a linear relationship with the amplitude of deformation, reflecting what is known as the linear viscoelastic regime. When a polymer filled with nanoparticles undergoes constant deformation, within the linear viscoelastic regime, the relaxation of its molecules is impeded by the presence of nanoparticles. This results in slower stress relaxation and increased material elasticity. Figure 14 illustrates this phenomenon in the case of polystyrene (PS)/clay nanocomposites [129]. In this case, the stress relaxation modulus, G(t), which is the stress divided by the amplitude of the deformation imposed to the material, is depicted for three samples of PS with respectively 0, 3.5 and 9.5wt % clay nanoparticles. Adding clay to the polymer significantly slows its stress relaxation.

This slower stress relaxation is attributed to what is known as **rheological percolation**. This phenomenon occurs for concentrations of nanoparticles that are high enough to impede the relaxation of the macromolecules. The concentration at which this phenomenon begins, referred to as the rheological percolation threshold, is typically lower [66, 67, 112, 130] than the electrical percolation threshold as the particles do not need to be in contact to prevent the movement of macromolecules, unlike the requirement for electrical conduction, as schematically illustrated in Figure 15. However, it can give very useful insights about the formation and the evolution of conductive particles networks when CPC materials are subjected to deformation in the molten state.

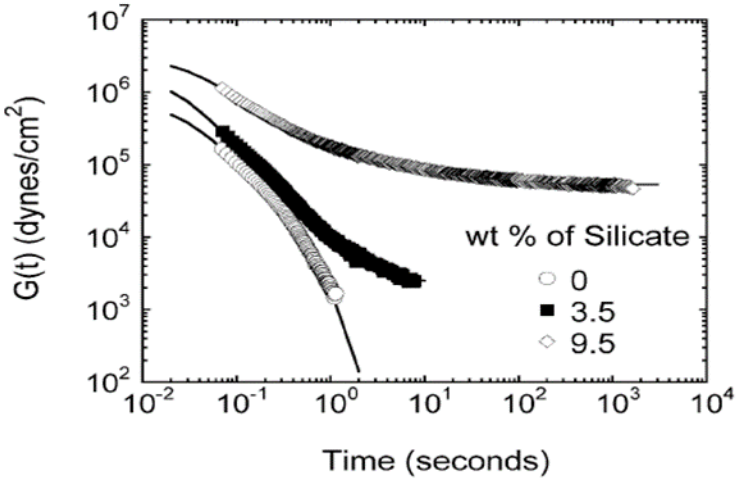

Figure 14: Time dependence of the linear stress relaxation modulus G(t) at 85 °C for the unfilled PS and PS nanocomposites containing respectively 3.5 and 9.5 wt% silicate
Reprinted with permission from reference [129]

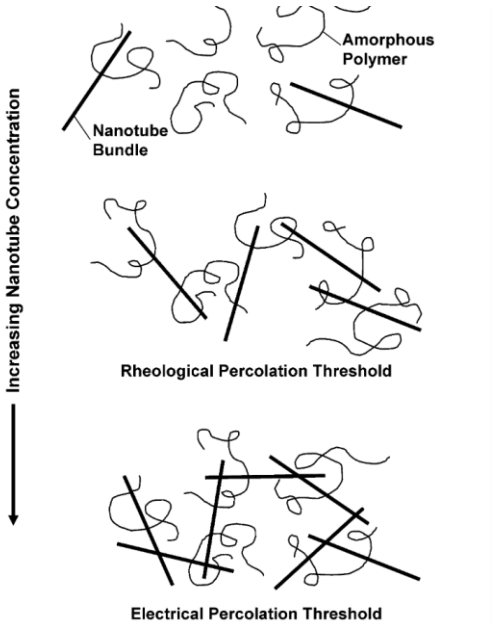

Figure 15: Illustration of electrical percolation threshold and rheological percolation threshold in polymer/CNT nanocomposites
Reprinted with permission from reference [130]

The rheological percolation threshold is typically determined by assessing the rheological behavior of nanocomposites under small amplitude oscillatory shear (SAOS) at different nanoparticles concentrations. Figure 16 depicts the rheological behavior of nanocomposites of styrene ethylene butadiene styrene (SEBS) with varying amounts of MWCNT, subjected to small amplitude oscillatory shear [16]. By plotting the storage modulus of the materials against nanoparticle concentration, at low frequencies like 0.05 rad, a sigmoidal curve similar to Figure 1 is obtained. This allows for the evaluation of the rheological percolation threshold concentration using the power-law equation (1), similar to how the electrical percolation threshold concentration is determined.

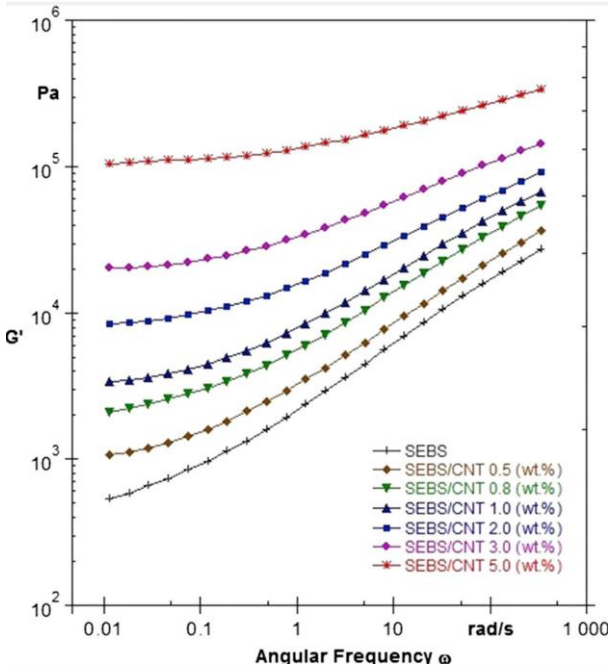

Figure 16: Storage modulus G′ as a function of frequency of neat SEBS and SEBS/CNT nanocomposites at different CNT weight fractions
Reprinted with permission from reference [16]

2-2) Simulation of the evolution particle network during processing and post-treatment

Achieving a low percolation threshold concentration through the optimization of the CPC composition, morphology and conductive networks configuration as discussed above, does not necessarily halt its morphological evolution. Instead, the percolation threshold is dynamic and can vary if the CPC material is subjected to a post-treatment such as thermal annealing at a temperature above the melt or softening point of the polymer matrix or to a further processing. A simple thermal annealing could result in a change of electrical properties of CPC, containing graphene, CNT or CB particles, as illustrated in Figure 17. The change of electrical properties is attributed to redistribution of conductive networks due to various reasons highlighted in previous sections, mainly: diffusion and migration of conductive particles, coarsening of blend morphology for double percolation type materials, change in the crystalline structure of the polymer matrix or in some cases the application of an external field treatment such as an electric field [31, 45, 58, 60, 114, 131, 132].

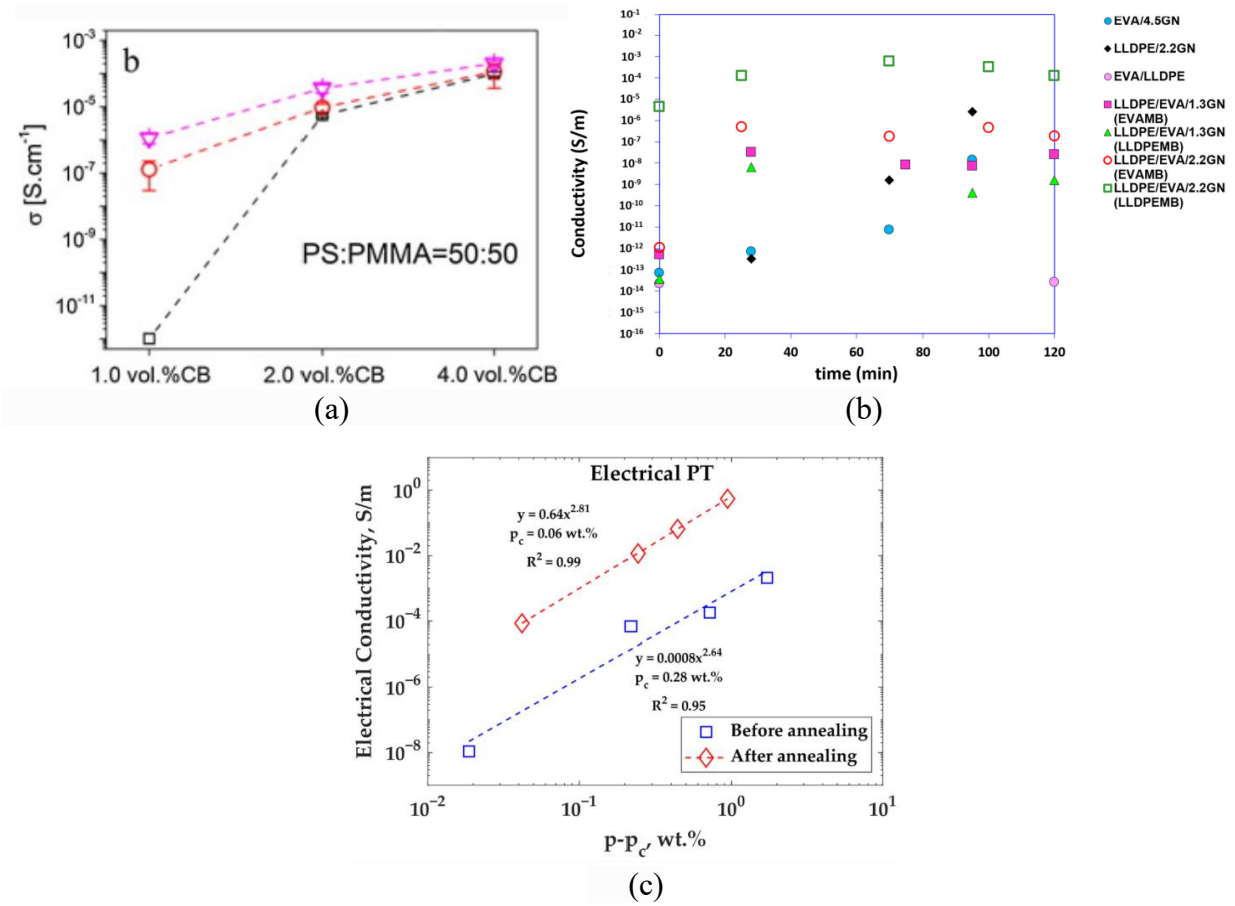

Figure 17: (a) Dependence of electrical conductivity on CB content for PS/PMMA/CB composites annealed at 200 °C for different times: squares: 0 mins, circles: 30 min; triangles: 120 min (reprinted with permission from reference [31]), (b) Dependence of room temperature electrical conductivity of EVA/GnP, LLDPE/GnP and LLDPE/EVA/GnP nanocomposites with different GnP concentrations, annealed at 160 °C up to 120 minutes (reprinted with permission from reference [45]) and (c) power-law fitting and experimental data of electrical conductivity of PP/PS/MWCNT nanocomposites before and after annealing at 200 °C versus reduced filler content ($\rho - \rho_c$) (reprinted with permission from reference [60])

2-2.1) Thermal annealing

To explain further the phenomenon, Kurusu et al.[114] and Helal et al.[58] used rheology as a tool to get insights of the evolution of morphology and explain the evolution of electrical properties of low linear density polyethylene (LLDPE), ethylene vinyl alcohol (EVA) and blends of the two polymers forming a co-continuous morphology to which graphene nanoplatelets had been added. For that, they subjected the materials to time sweep tests at 160° C (above melting temperature of both polymers) using a rotational rheometer and evaluated the evolution of the storage modulus at a frequency of 0.1 rad.s^{-1}. In parallel they annealed the material in the hot press and evaluated the electrical conductivity as a function of annealing time. The findings depicted in Figure 18 and Figure 18(b) revealed an interesting trend. While the storage modulus and electrical conductivity of the single-phase polymer composites, i.e. LLDPE/GnP and EVA/GnP, exhibited a steady

increase during annealing, the behavior differed for the LLDPE/EVA/GnP blends. In the case of the blends, both the storage modulus and electrical conductivity reached a plateau after approximately 30 minutes, indicating a stabilization in morphology. The increase of storage modulus and electrical conductivity was attributed to both a coarsening of the blend morphology and a migration of the graphene to the interface between the polymers, as also observed by Bai et al.[115]. However, and despite employing a superposition principle intended to decouple the effects of blend morphology and conductive particles network evolution, pinpointing the exact cause of this stabilization remained challenging.

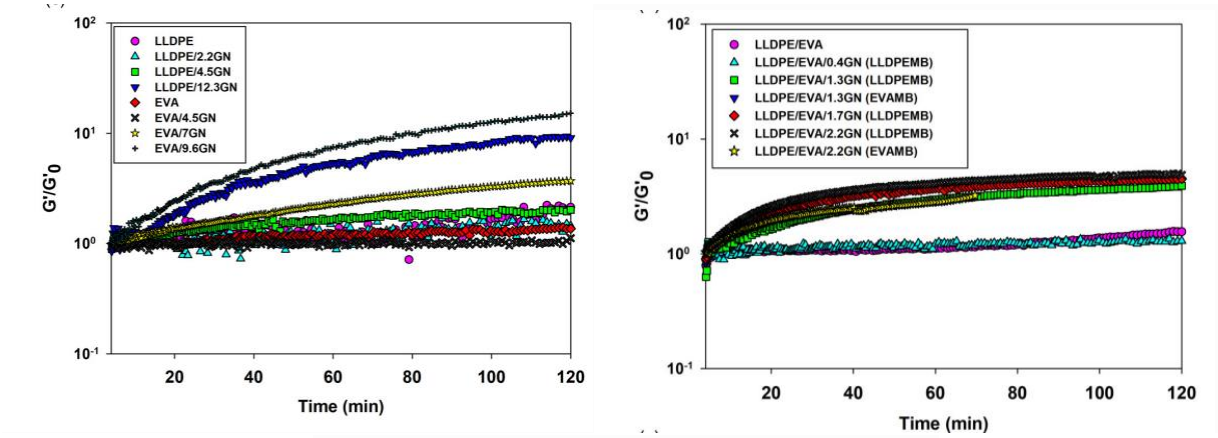

(a) (b)

Figure 18: Evolution of storage modulus G' of LLDPE/GnP, EVA/GnP and LLDPE/EVA/GnP nanocomposites annealed at 160 °C as function of annealing time: (a) LLDPE/GnP and EVA/GnP and (b) LLDPE/EVA/GnP
Reprinted with permission from reference [58]

Strugova et al.[60] conducted similar studies, working with a tailored blend of polypropylene/polystyrene (PP/PS) to which multiwall carbon nanotubes (MWCNT) had been added. In their study, they performed a combined rheological and electrical characterization of the blend using a MCR501 Anton Paar rheometer equipped with a dielectro-rheological device (DRD with ST2826/A high-frequency LCR meter). They subjected the blend to a sequence of small amplitude oscillatory shear (SAOS), thermal annealing, and SAOS, as shown in Figure 19 and evaluated the evolution of their rheological and electrical behaviors.

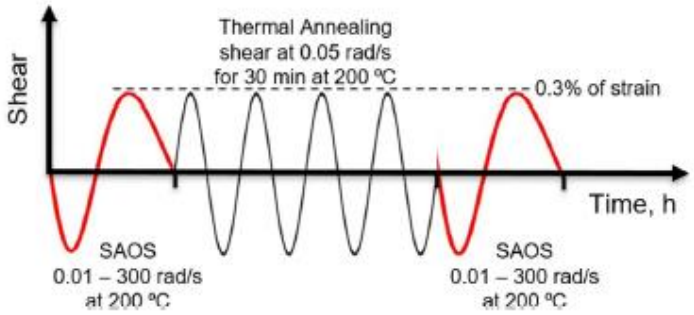

Figure 19: experimental protocol consisting of a sequence of SAOS, followed by a time sweep (simulating thermal annealing), followed by another SAOS, to evaluate the evolution of CPC morphology during thermal annealing
Reprinted with permission from reference [60]

Figure 20 depicts the evolution of the electrical conductivity and storage modulus of the PP/PS/MWCNT blends studied during annealing. The results demonstrate similarities to those observed by Helal et al. [58], in terms of the evolution of electrical conductivity and storage modulus G' with annealing time. To determine whether the change in electrical conductivity was attributable to a change in blend morphology or to the evolution of MWCNT network, the researchers modeled the behavior of the SAOS data before and after annealing, respectively. They utilized a modification of the theory proposed by Yu et al. [133], which predicts the SAOS behavior of polymer blends with co-continuous morphology. This modified model establishes a relationship between the rheological behavior of a co-continuous morphology blend subjected to SAOS, the rheological behavior of the pure component and the interfacial area between the polymers. Through their analysis, they observed that thermal annealing of the blend nanocomposites led to a maintained or slightly more refined co-continuous morphology and a reduction of electrical percolation threshold by over 70% due to the migration of MWCNT to the PP/PS interface. The presence of higher fraction of kinetically trapped MWCNT at the interface helped to prevent the coalescence and coarsening of the blend morphology, as compared to unfilled PP/PS blend which exhibited significant increase of its characteristic domain size after thermal annealing.

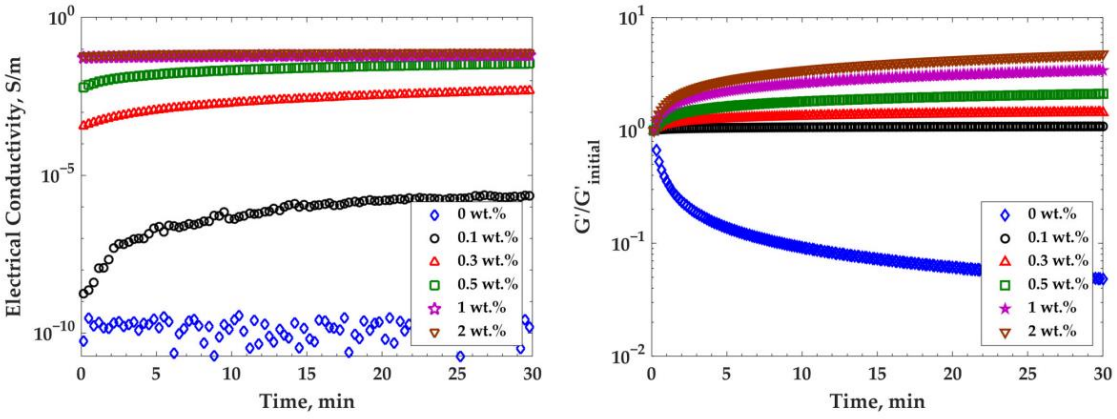

(a) **(b)**

Figure 20: (a) electrical conductivity as a function of annealing time for PP/PS/MWCNT with different concentrations measured at 20 Hz and 200 °C, (b) time dependent evolution of storage modulus (G') at 200 °C

Reprinted with permission from reference [60]

2-2.2) Steady shear deformation

Besides thermal treatment present in annealing thermo-mechanical stresses, often encountered during melt processing of polymers, blends and their (nano)composites, can induce ongoing changes in their respective morphologies and, therefore, on their functional properties. It is therefore essential to understand how morphology of materials, particularly blends, evolves when subjected to such conditions. Unfortunately, when deformations become rapid and large, corresponding to those typically encountered during melt processing, the material's rheological behavior enters the nonlinear regime, where conventional constitutive equations may not apply, and it is not easy to predict the evolution of morphology.

Using the same approach as in their prior study, Strugova et al. [61] subjected PP/PS/MWCNT blend nanocomposites to a sequence of SAOS, steady shear and SAOS to assess the impact of steady shear deformation on the co-continuous PP/PS blend's morphology, MWCNT conductive network, and resulting electrical conductivity. They observed that the evolution of the blend morphology and MWCNT network depended on the magnitude of shear strain, shear rate and MWCNT concentration. More specifically, when the MWCNT concentration reached a level high enough to fully cover the interface, the morphology and conductive particle network were stabilized. However, if the concentration of MWCNT is slightly below this critical threshold, the morphology tends to coarsen and the electrical network is disrupted, although total restoration is possible through thermal annealing or stress relaxation. Conversely, when the concentration of MWCNT is significantly lower than the interface coverage threshold, total recovery from the disruptive effect of applied shear strain and rate cannot be achieved. Figure 21 gives a schematic summary of their findings.

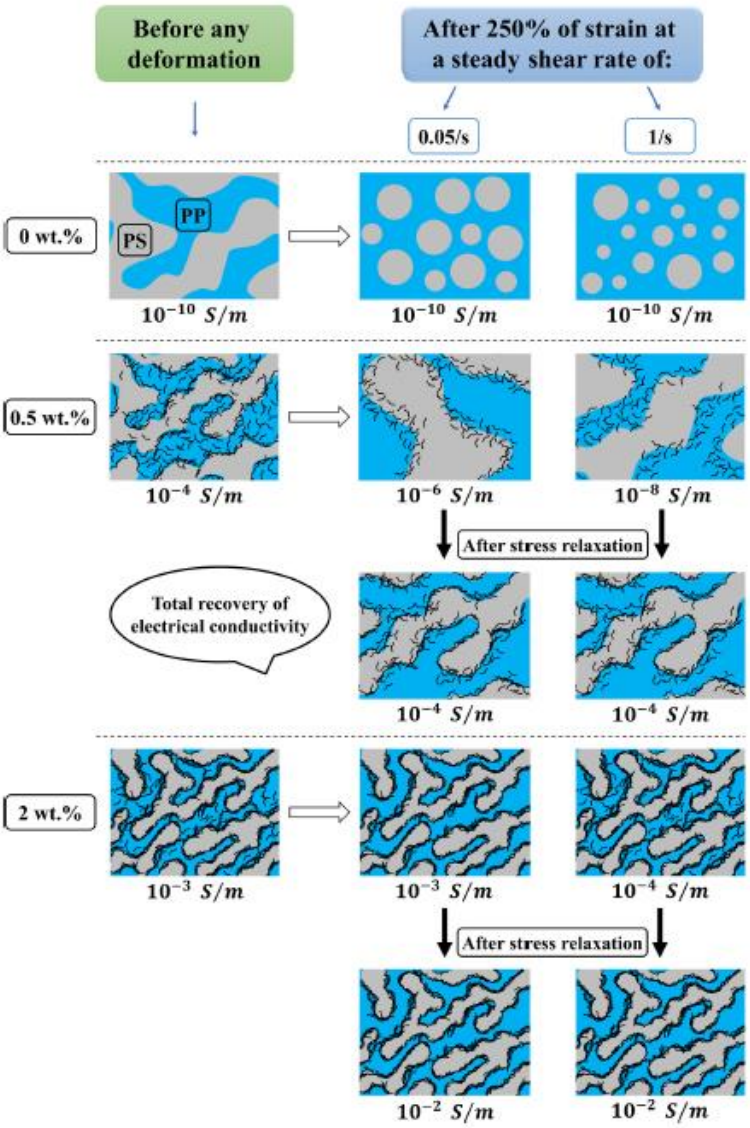

Figure 21: effect of steady shear deformation at different shear rates and stress relaxation on the morphology and electrical conductivity of co-continuous PP/PS blends containing different MWCNT loadings
Reprinted with permission from reference [61]

Similar trends were obtained by Kou et al. [56] who worked with co-continuous blends of PLA/EVA to which GnP had been added. At 0.5 wt% GnP, a concentration well above the percolation threshold estimated at 0.048 wt. %, they concluded that the interfacial GnP network and the electrical conductivity recover with thermal annealing after nonlinear deformation, as illustrated in Figure 22. They also found that the electrical conductivity is maintained during 2-10 mins melt compounding (Figure 6(b)), a relatively large range, suggesting that GnP form robust networks capable of maintaining the original electrical conductivity of the blends during subsequent melt processing. This robustness is related to the higher interfacial stability of GnP and

particles with 2D geometry in general, compared to CNT (1D) and CB (0D), according to the slim-fast mechanism [118, 134].

It is worth noting that the shear rates at which Strugova et al.[61] and Kou et al. [56] subjected their blend nanocomposites are much lower than the ones typically encountered during melt processing and therefore more research should be carried out in this direction.

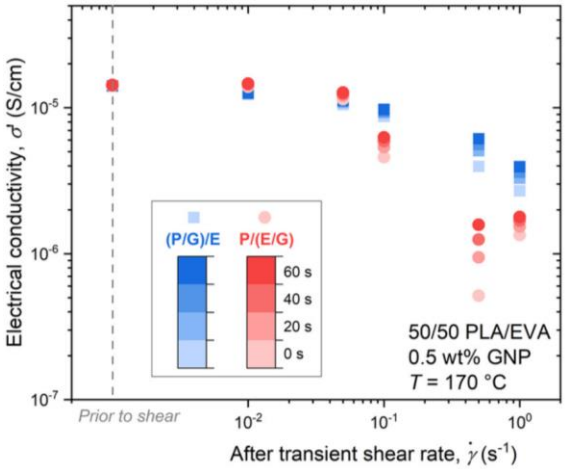

Figure 22: Evolution of the electrical conductivity of PLA/EVA blend containing 0.5 wt.% GnP after transient shear at different rates and stress relaxation
Reprinted with permission from reference [56]

III- Recycling of CPC

3-1) Main routes of plastics recycling: review

Plastics recycling has been extensively investigated during the last decades due to the pressing need to increase plastic recycling rates and to adopt circular approaches in the management of plastics waste. The main recycling routes that have been investigated are mechanical recycling and chemical recycling [135, 136]. Mechanical recycling presents lower carbon footprint, and impact on the environment as well as lower cost, compared to the other recycling processes [136, 137]. It consists of crushing or shredding plastic parts at the end-of-life followed by a fine grinding into smaller pieces. These pieces can be ultimately used to manufacture the same product (closed-loop recycling) or a different product (open-loop recycling) by using standard plastic manufacturing processes, such as extrusion, injection molding and/or compression molding. However, one major challenge of mechanical recycling is the thermo-mechanical and thermo-oxidative degradation suffered by most thermoplastics during their melt reprocessing. In fact, the temperatures and shear rates at which the polymers are melt processed, during extrusion for example, result in molecular degradation and associated changes in material's properties. This issue becomes even more relevant in the context of extensive or repeated mechanical recycling. Therefore, extensive mechanical recycling of plastics, particularly polyolefins, has been experimentally simulated by performing multiple extrusion cycles [138, 139]. In addition to unfilled thermoplastics, repeated mechanical recycling of thermoplastic composites reinforced with fibers and particle fillers such as talc and fumed silica has been investigated in several studies. Typically, these studies report the effects of repeated reprocessing steps on the structure and thermo-mechanical properties [138,

140]. Besides standard mechanical recycling or reprocessing, possible strategies for recycling or improving the sustainability of thermoplastic composites include partial using recycled polymer matrices with virgin filers or recycled fillers recovered from waste such as ground tyre rubbers [141] and post-used carbon fiber thermoset composites [142].

In the following sections, recycling of carbon nanomaterials-based CPC will be discussed. Focus will be limited to mechanical recycling due to its relevance.

3-2) Recycling of carbon nanomaterials-based CPC

Similar to unfilled thermoplastics and other thermoplastic composites, mechanical recycling of CPC involves the challenges associated with the thermo-mechanical and thermo-oxidative degradation of thermoplastic matrices. An additional major consideration, specific to this class of materials, is the evolution of conductive filler networks during processing which depends on multiple factors related to the intrinsic characteristics of the conductive filler and thermoplastic matrix as well as to the processing/reprocessing conditions, as discussed in the previous sections of this chapter. As the electrical conductivity of CPC is strictly governed by the conductive filler networks, all these factors must be taken into consideration in the mechanical recycling of CPC and in the design/development of new recyclable CPC.

Our review of current literature on fully recyclable carbon nanomaterials-based CPC revealed a predominant focus on case studies involving flexible conductive thermoplastic or thermoplastic elastomer composites. These studies primarily employ mechanical recycling strategies [8, 11, 143-145]. Flexible CPC commonly utilize polymer matrices such as Thermoplastic Polyurethane (TPU), Styrene-Butadiene Rubber (SBR), and Poly(Styrene-Ethylene-Butadiene-Styrene) Rubber (SEBS). As this category of CPC is particularly relevant for strain sensing applications and flexible electronic devices, the recycling investigations delve into the evolution of electrical, mechanical, and, in some instances, sensing properties after several recycling cycles. The recycling process typically involves shredding and grinding the CPC material, followed by reprocessing via compression or injection molding.

For instance, in the studies of Dong et al. [143] and Yan et al. [144] , PU/MWCNT nanocomposites, with CNT loadings in the range 3 to 7 wt.%, were mechanically recycled by cutting into small pieces and remolding using the hot press. This cycle was repeated multiple times. The evaluation of mechanical properties and electrical conductivity was performed at each cycle and revealed that these properties can be restored for at least 3 reprocessing cycles, as illustrated in Figure 23. Following the same recycling procedure, Shen et al.[11] studied the recycling of SEBS/GnP composites featuring initially a segregated structure and a low percolation threshold around 0.3 vol.% GnP. They found that the electrical conductivity of the composite containing 1.1 vol.% GnP was maintained up to 3 recycling cycles and concluded that the segregated structure was well-recovered in the recycled composites. In another study by Stan et al.[145], the recycling of injection molded low-density polyethylene (LDPE)/MWCNT nanocomposites containing 0.5 up to 5 wt.% MWCNT was investigated. Shredding and injection molding were adopted for reprocessing. The authors reported as well minimal or no reduction of the electrical and rheological properties after one recycling cycle and concluded that these composites can undergo multiple

reprocessing cycles. Furthermore, compared with the virgin composites, the recycled composites exhibited a significant increase of strain at break up to 30%, especially for MWCNT loadings higher than 1 wt.%. Tensile and tensile modulus were improved as well but a lower extent. The authors attributed the improvement of mechanical properties in the recycled materials to a better polymer/CNT interface due to a partial breakage of the secondary agglomerates of CNT during recycling, without affecting the electrical conductivity.

It is worth noting that, in most of the above-mentioned studies, conductive composites featured originally a random spatial distribution of the conductive particles. Also, the loadings of conductive particles in the composites selected for the recycling evaluation are well above the percolation threshold. These two conditions facilitate the reconstruction of the conductive networks during reprocessing, in a state akin to the original composites.

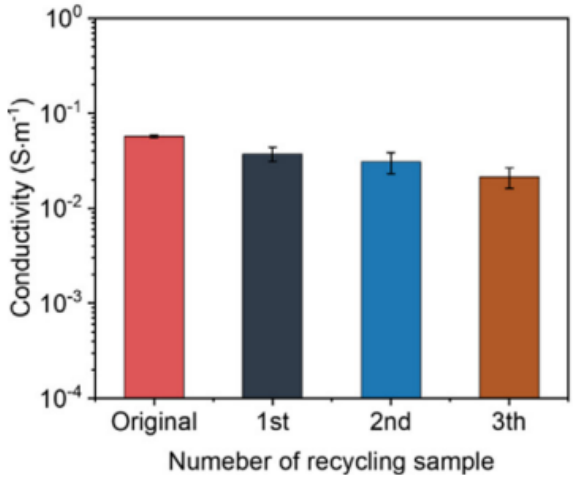

Figure 23: Evolution of the electrical conductivity of PU/MWCNT composite after multiple recycling cycles
Reprinted with permission from reference [143]

Another relevant strategy aiming at improving the environmental sustainability of CPCs is based on the use of recycled thermoplastic matrices melt compounded with virgin or recycled conductive fillers to develop new CPCs. In the particular, studies of Rahaman et al.[146] and Lu et al. [29] have investigated respectively the use of recycled polyethylene (mixture of LDPE and LLDPE grades) and blends of recycled HDPE with polylactic acid (PLA) as matrices for CB containing CPCs. The new CPCs were respectively fabricated by solvent mixing and melt compounding and exhibited electrical and mechanical properties adequate for use in ESD and EMI shielding applications, among others. However, it is worth noting that the processability and properties of these materials were not compared to counterparts obtained with virgin polymers and the evolution of their performance after reprocessing has not been evaluated. In an analogous approach, recycled conductive fillers, such as graphite powders recycled by simple chemical and thermal processes from electric discharge machining electrode scraps and anode materials from lithium-ion batteries, are combined with virgin or recycled polymer matrices to produce new CPCs [147, 148]. An example of this approach, reported by Jena et al. [148], is illustrated in Figure 24, where recycled graphite was melt compounded with HDPE using a twin-screw extruder. Then, the resulting

composites were injection molded. In this study, CPCs obtained with the reclaimed graphite exhibited the same level of electrical conductivity compared to those fabricated with commercial graphite. Moreover, higher elongation at break and tensile strength were achieved and attributed to a better dispersion of the recycled graphite compared to the commercial graphite in the HDPE matrix due to possible formation of functional groups during the graphite reclaiming process.

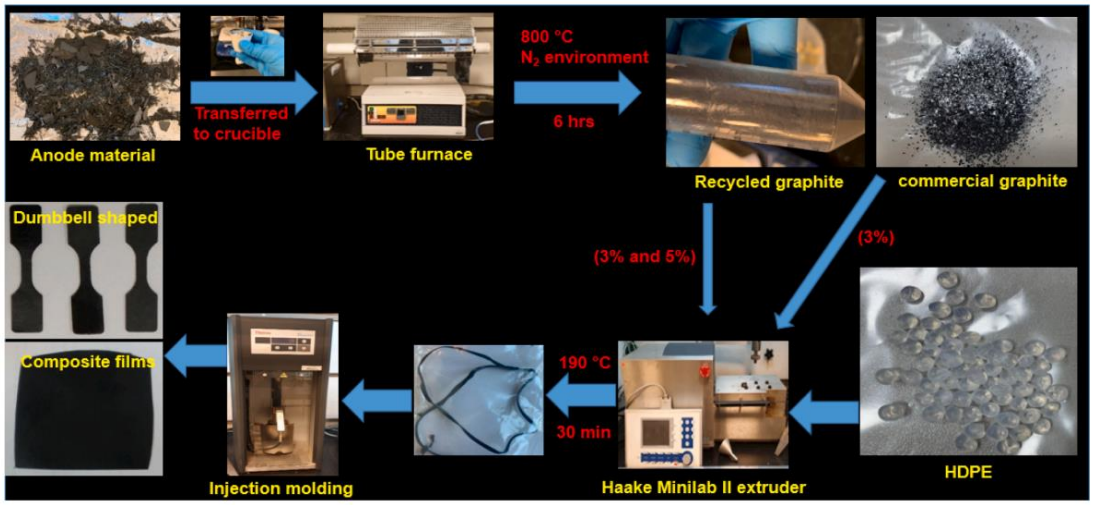

Figure 24: Steps involved in the fabrication of HDPE composites containing recycled graphite from anode materials
Reprinted with permission from reference [148]

Although they are not equivalent to fully recyclable CPCs and do not directly address closed-loop or repeated recycling, strategies based on use of recycled polymer matrices and/or recycled conductive fillers to develop new CPCs enable two significant advantages: 1) reduction of the environmental impact associated with the manufacturing of CPCs through the use of recycled materials, and 2) flexibility to use the typical approaches to tune conductive networks and achieve low percolation thresholds such as polymer blends with controlled morphology, segregated structures, hybrid fillers…

Recently, more holistic approaches to address the end-of-life of devices comprising CPCs, such energy harvesting and energy storage devices, have been investigated. Among them, the recent study by Di Persio et al.[149], which proposes mechanical, thermal and chemical-based approaches to recover and recycle valuable materials used in piezoelectric and thermoelectric generators. In particular, they discuss the recycling of one type of CPC present in such devices, namely: Polyether ether ketone (PEEK)/SWCNT composites which are used to make thermoelectric composite legs. The simplest suggested approach to recycle these materials is based on mechanical recycling by melt compounding, with potential addition of virgin PEEK, SWCNT or additives such as polyethylene glycol, to tailor the properties of the reprocessed composite.

3-3) Effect of conductive nanomaterials on recyclability and multifunctional properties of CPC

In general, the approach of upgrading the functional properties of recycled polymers using nanoparticles is a widely acknowledged avenue and has been extensively investigated by researchers in the last years [50-52, 150-156]. Different nanofillers, such as nanoclays, nano silica, nano $CaCO_3$ and carbon-based nanomaterials, have been applied to different recycled polymers, especially packaging plastics such as PET, PP, PE, PS, etc. The addition of nanoparticles resulted in enhancements of a wide range of properties including mechanical reinforcement, thermal stability, barrier properties and processability, to name a few.

In CPC materials, carbon-based nanomaterials as a class of nanomaterials, bring in addition to the desired improvement of electrical conductivity, several benefits, as expected. Some of these additional benefits are of particular interest, in the context of recyclable CPC or CPC made from recycled materials.

More precisely, improvement of thermal stability of the polymer matrix is an advantage widely observed when adding different types of carbon nanomaterials to thermoplastic matrices. In Figure 25, thermograms of PP/CB and PP/GnP subjected to thermogravimetric analysis (TGA) at constant heating rate of 10 °C/min reveal the shift of thermal degradation toward higher temperatures with increasing loading of GnP or CB. This improved thermal stability allows better protection of the virgin and recycled polymer matrices during reprocessing/recycling, which can translate in a higher number of recycling cycles without loss of properties [12, 29, 146-148].

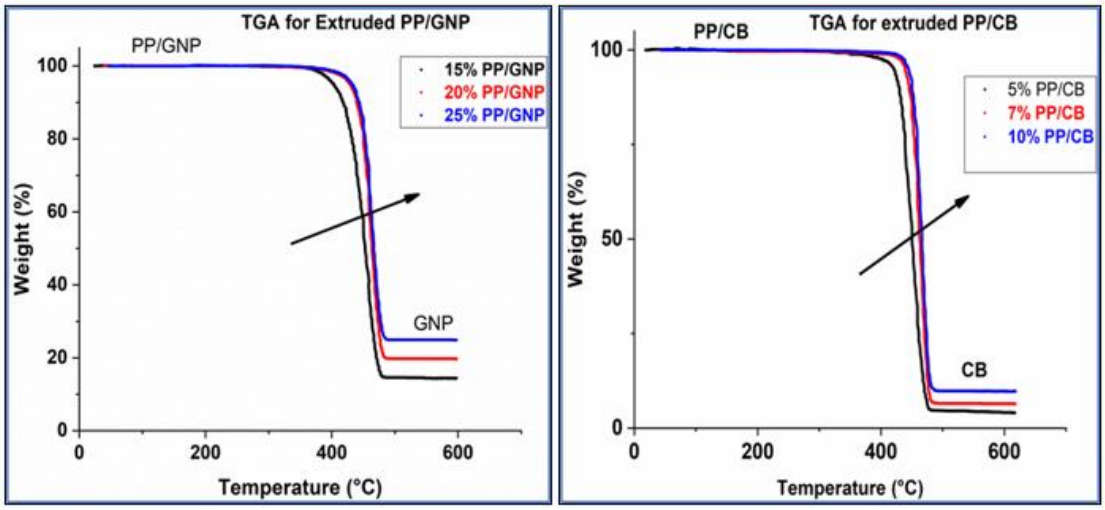

(a) (b)

Figure 25: effect of conductive particles on the thermal degradation behavior of PP matrix at different loadings, (a) CB and (b) GnP (Courtesy of MSc student Omayma Belgacem)

In the context of recyclability and processability, another interesting property, characteristic of some carbon-base particles such as graphite, graphene and their derivates, is the process aid effect. In fact, when added at low loadings and featuring certain dispersion states, particles with 2D geometry may facilitate the flow of molten polymer resulting in a viscosity decrease and easier

processing, which also translates in lower thermo-mechanical stress and less extent of thermal degradation. Recently, Genoyer et al. [46] investigated, through a rheological study, the effectiveness of different graphene grades as processing aids in molten polystyrene (PS). They observed a maximum decrease of viscosity, up to 29%, at 2 wt.% graphene loading, and that the efficiency of this process aid effect is strictly dependent on the presence of secondary agglomerates. They concluded that this effect is attributed to the phenomenon of superlubricity, which is a lubricating mechanism that is closely linked to the atomic structure of the particles and to the angles between the agglomerated flakes, as proposed by Ferreira et al. [157].

Besides properties related to reliability and processability, carbon-based nanomaterials can act as photo-stabilizers and physical barriers, protecting polymer matrices from weathering and agents, such as oxygen and water, contributing to their accelerated degradation during use [21, 48, 49, 158, 159]. In particular, carbon-based nanomaterials feature a combination of photo-stabilization mechanisms, mainly: UV absorption and free radical scavenging [49, 160].

At last, nanoparticles have the potential to act as non-specific compatibilizers for polymer blends, allowing to stabilize their morphologies. Nanoparticles compatibilization mechanisms are attributed to their alteration of the viscosity ratio and mainly to their migration at the polymer-polymer interface, thereby preventing coalescence [56, 61, 124, 161-169]. As seen in the previous section when discussing CPC systems based on polymer blends, nanoparticles interfacial localization depends on various factors: thermodynamics, kinetic aspects related to processing and mixing, as well as nanoparticles attributes like surface chemistry and geometry. Besides, nanoparticles with 2D geometry, such as graphene and its derivates, are expected to exhibit more interfacial stability due to their slow migration rate and adaptability to interfaces [56, 170]. Also, nanoparticles loadings higher than a critical threshold for full interface coverage, which is higher than the electrical percolation threshold, are needed to ensure stability of the interfacial network and of the electrical conductivity [56, 61]. Hence, in the case of double percolated CPC systems based on co-continuous polymer blends, carbon-based nanoparticles are expected to play a dual role: 1) conductive filler and 2) compatibilizer, enabling and facilitating the reprocessing of this class of multiphase polymer CPC, while maintaining their morphology and functional properties. Furthermore, the compatibilizer role of nanoparticles allows to consider mixed plastic waste streams, a class of plastic waste typically directed to landfilling, in the development of CPCs. In this context, studies on the use of graphene to valorize recycled HDPE and mixed polyolefins waste streams have been recently published by Sultana et al. [50, 52] and Diallo et al. [51].

However, the compatibilizing efficiency of bare or pristine nanoparticles is typically limited. To promote nanoparticles localization and stability at polymer blend interfaces and increase their compatibilization efficiency, it is possible to tune their affinity to the polymer phases via surface modification [171, 172]. This step increases their interfacial interactions with the polymer phases. Commonly reported strategies to endow reactive groups on inorganic nanoparticles is via silane coupling agent [172, 173]. Other strategies such as grafting molecular chains of each polymer component to the surface of nanoparticles to obtain Janus nanoparticles might be more complex and blend specific [174]. In addition, some surface modifications might alter the alter the electrical properties [175].

3-4) Additive manufacturing of CPC as a circular process for CPC

Material extrusion-based additive manufacturing (MatEx AM) processes, such as Fused Filament Fabrication (FFF), are known for their efficiency in terms of material and energy consumption. The recent trend in MatEx AM research is focused on using recycled plastics or composites based on recycled plastic matrices, as 3D printing feedstocks. Also, the development of large-scale 3D printers and pellet 3D printers is promoting further the use of recycled plastics in these processes and their integration simultaneously as manufacturing and recycling strategy, in the aim of enhancing circularity and decentralizing plastic waste recycling [176-184]. In this context, some recent studies investigated the effect of thermomechanical treatment through repeated recycling involving filament extrusion and 3D printing or direct pellets 3D printing, on the mechanical performance, thermal behavior and printability of different plastics [181]. Most of these studies reported overall maintained mechanical properties and printability after several recycling cycles.

From another front, MatEx AM is also attractive for CPCs. It allows significant design flexibility, compared to conventional manufacturing processes, to fabricate complicated geometry components namely for applications such as sensors and flexible electronics [4, 5, 9, 12, 15, 185-192]. The thermoplastic matrices that have been investigated in these studies, include: TPU, ABS, PP. PLA and PBT. CB, CNT and graphene materials have all been investigated as conductive fillers as well. Overall, ranges of conductivity like those obtained by CPC conventional manufacturing methods were successfully achieved. However, difficulty in incorporating high loadings of some conductive fillers, mainly CNT, and 3D printing constrains, such as slow print speeds and low resolution have been reported [185]. It is worth noting that the cited studies are related to CPC manufactured by FDM or pellet 3D printing. Other AM techniques such as Selective laser sintering (SLS) or Direct Ink Writing (DIW) have been investigated for the fabrication of CPCs. They were not considered in this discussion since they are less relevant to the context of recycling.

The use of recycled polymer matrices in 3D printing of CPCs has not been extensively investigated. A recent study by Stan et al.[12] investigated the printability and piezoresistive behavior of recycled TPU(rTPU)/CNT vs. virgin TPU(vTPU)/CNT conductive nanocomposites containing up to 5 wt.% CNT. Initially, both types of nanocomposites were extruded to obtained filaments, which were 3D printed into samples with different infill orientations. The characterization of the mechanical properties and electrical conductivity of both types of nanocomposites revealed that their mechanical and electrical performance is comparable. However, the addition of 5 wt.% CNT to both types resulted in a significant decrease of elongation at break compared to unfilled TPU, which can be a limiting factor for repeated recycling of TPU/CNT nanocomposites.

Conclusion

The advancement of conductive polymer composites (CPCs) brings with it challenges and opportunities in terms of processability, recyclability, and durability. With the increasing pressure for recycling and distributed recycling and the growing demand for sustainable production, several key considerations emerge.

One crucial area for future research is the identification and evaluation of techniques to mitigate polymer degradation and improve the properties of reprocessed/recycled thermoplastics and their (nano)composites within the context of distributed recycling. In the context of CPCs, this also includes addressing the challenge of maintaining low and ultra-low percolation thresholds without compromising optimized conductive network structures and electrical conductivity.

Achieving low percolation thresholds depends on various factors such as: 1) content, geometry and surface chemistry of the conductive nanofillers, 2) affinity between the nanofillers and polymer matrices, 3) rheological properties of the polymer matrices as well as 4) processing techniques and parameters.

While literature is still limited on the topic CPCs recycling, the current studies indicate that CPCs with conductive nanoparticles loadings well above the percolation threshold can be recycled mechanically up to a few cycles without significant loss of their electrical conductivity or other physical properties. The presence of robust network structures at nanofillers above the percolation threshold ensures their maintenance/easy reconstruction during the recycling process. Hence, designing CPCs with balanced loadings of conductive fillers, well above the percolation threshold but without significant processing challenges and increased costs, can be one way to ensure their recyclability at their end-of-life.

CPCs with low/ultra-low percolation thresholds and tailored/complex conductive networks, such as those achieved through segregated structures and double percolated multiphase polymer blends, may pose higher challenges in maintaining their conductive networks and conductivity post-recycling. However, available literature suggests that mild recycling processes like shredding and compression molding can preserve the original conductive structure in CPCs featuring segregated networks.

In the case of CPCs fabricated from polymer blends, the selective localization of conductive nanoparticles with specific geometries and surface chemistries at blend's interfaces enhances their role as both conductive fillers and blend compatibilizers. This dual functionality not only improves mechanical recycling but also opens avenues for integrating mixed plastic waste streams into CPC development. In this context, conductive nanofillers with 2D geometry might be of particular interest due to their better stabilization at the interface and slow migration rates.

Finally, as we move forward, considerations for recycling existing CPCs and designing new ones with recycling in mind will be paramount. Therefore, understanding CPCs' behavior under different recycling scenarios, through appropriate rheological characterization will provide valuable insights for more sustainable and efficient production and recycling practices, especially when integrated with additive manufacturing technologies.

References

1. Siwal, S.S., et al., *Carbon-Based Polymer Nanocomposite for High-Performance Energy Storage Applications.* Polymers, 2020. **12**(3): p. 505.
2. Paleo, A.J., et al., *Thermoelectric properties of polypropylene carbon nanofiber melt-mixed composites: exploring the role of polymer on their Seebeck coefficient.* Polymer Journal, 2021. **53**(10): p. 1145-1152.

3. Panahi-Sarmad, M., et al., *A Comprehensive Review on Carbon-Based Polymer Nanocomposite Foams as Electromagnetic Interference Shields and Piezoresistive Sensors.* ACS Applied Electronic Materials, 2020. **2**(8): p. 2318-2350.
4. Liu, F., et al., *Additive Manufacturing of Stretchable Polyurethane/Graphene/Multiwalled Carbon Nanotube-Based Conducting Polymers for Strain Sensing.* ACS Applied Nano Materials, 2023. **6**(6): p. 4522-4531.
5. Xiang, D., *Carbon-Based Conductive Polymer Composites: Processing, Properties, and Applications in Flexible Strain Sensors* 2023: CRC Press.
6. Kaplan, M., B. Krause, and P. Pötschke, *Polymer/CNT Composites and Filaments for Smart Textiles: Melt Mixing of Composites.* Solid State Phenomena, 2022. **333**: p. 91-96.
7. Mu, Q., et al., *The Effect of Filler Dimensionality and Content on Resistive Viscoelasticity of Conductive Polymer Composites for Soft Strain Sensors.* Polymers, 2023. **15**(16): p. 3379.
8. Tao, X., S. Liao, and Y. Wang, *Polymer-assisted fully recyclable flexible sensors.* EcoMat, 2021. **3**(2): p. e12083.
9. Zhang, Z., et al., *Effect of Carbon Black on the Strain Sensing Property of 3D Printed Conductive Polymer Composites.* Applied Composite Materials, 2022. **29**(3): p. 1235-1248.
10. Sharma, S., et al., *Recent progressive developments in conductive-fillers based polymer nanocomposites (CFPNC's) and conducting polymeric nanocomposites (CPNC's) for multifaceted sensing applications.* Journal of Materials Research and Technology, 2023. **26**: p. 5921-5974.
11. Shen, Z. and J. Feng, *Mass-produced SEBS/graphite nanoplatelet composites with a segregated structure for highly stretchable and recyclable strain sensors.* Journal of Materials Chemistry C, 2019. **7**(30): p. 9423-9429.
12. Stan, F., I.-L. Sandu, and C. Fetecau, *Investigation on the Printability of Recycled Thermoplastic Polyurethane/Carbon Nanotube Nanocomposites.* Journal of Manufacturing Science and Engineering, 2023. **146**(1).
13. Hussain, K.K., et al., *Exploring Different Carbon Allotrope Thermoplastic Composites for Electrochemical Sensing.* ACS Applied Polymer Materials, 2023. **5**(6): p. 4136-4145.
14. Deng, H., et al., *Progress on the morphological control of conductive network in conductive polymer composites and the use as electroactive multifunctional materials.* Progress in Polymer Science, 2014. **39**(4): p. 627-655.
15. Jalali, A., et al., *Recent progress and perspective in additive manufacturing of EMI shielding functional polymer nanocomposites.* Nano Research, 2023. **16**(1): p. 1-17.
16. Kuester, S., et al., *Hybrid nanocomposites of thermoplastic elastomer and carbon nanoadditives for electromagnetic shielding.* European Polymer Journal, 2017. **88**: p. 328-339.
17. Kuester, S., et al., *Electromagnetic interference shielding and electrical properties of nanocomposites based on poly (styrene-b-ethylene-ran-butylene-b-styrene) and carbon nanotubes.* European Polymer Journal, 2016. **77**: p. 43-53.
18. Kuester, S., et al., *Processing and characterization of conductive composites based on poly(styrene-b-ethylene-ran-butylene-b-styrene) (SEBS) and carbon additives: A comparative study of expanded graphite and carbon black.* Composites Part B: Engineering, 2016. **84**: p. 236-247.
19. Huang, Y., et al., *Tailoring the electrical and thermal conductivity of multi-component and multi-phase polymer composites.* International Materials Reviews, 2020. **65**(3): p. 129-163.
20. Khan, J., S.A. Momin, and M. Mariatti, *A review on advanced carbon-based thermal interface materials for electronic devices.* Carbon, 2020. **168**: p. 65-112.
21. Ferreira Junior, J.C., et al., *Effects of an industrial graphene grade and surface finishing on water and oxygen permeability, electrical conductivity, and mechanical properties of high-density polyethylene (HDPE) multilayered cast films.* Materials Today Communications, 2022. **31**: p. 103470.

22. Xue, Q., *The influence of particle shape and size on electric conductivity of metal–polymer composites.* European Polymer Journal, 2004. **40**(2): p. 323-327.
23. Lin, L., et al., *Modified resistivity–strain behavior through the incorporation of metallic particles in conductive polymer composite fibers containing carbon nanotubes.* Polymer International, 2013. **62**(1): p. 134-140.
24. Luo, X., G. Yang, and D.W. Schubert, *Electrically conductive polymer composite containing hybrid graphene nanoplatelets and carbon nanotubes: synergistic effect and tunable conductivity anisotropy.* Advanced Composites and Hybrid Materials, 2022. **5**(1): p. 250-262.
25. Wu, S., et al., *Aligning multilayer graphene flakes with an external electric field to improve multifunctional properties of epoxy nanocomposites.* Carbon, 2015. **94**: p. 607-618.
26. Gong, S., Z.H. Zhu, and S.A. Meguid, *Anisotropic electrical conductivity of polymer composites with aligned carbon nanotubes.* Polymer, 2015. **56**: p. 498-506.
27. Lahaye, J. and G. Prado, *Morphology and Internal Structure of Soot and Carbon Blacks*, in *Particulate Carbon: Formation During Combustion*, D.C. Siegla and G.W. Smith, Editors. 1981, Springer US: Boston, MA. p. 33-55.
28. Lu, C., et al., *Triple percolation behavior and positive temperature coefficient effect of conductive polymer composites with especial interface morphology.* Polymer Bulletin, 2012. **68**(7): p. 2071-2087.
29. Lu, X., B. Kang, and S. Shi *Selective Localization of Carbon Black in Bio-Based Poly (Lactic Acid)/Recycled High-Density Polyethylene Co-Continuous Blends to Design Electrical Conductive Composites with a Low Percolation Threshold*. Polymers, 2019. **11**, DOI: 10.3390/polym11101583.
30. Mazaheri, M., J. Payandehpeyman, and S. Jamasb, *Modeling of Effective Electrical Conductivity and Percolation Behavior in Conductive-Polymer Nanocomposites Reinforced with Spherical Carbon Black.* Applied Composite Materials, 2022. **29**(2): p. 695-710.
31. Pan, Y., et al., *Enhancing the electrical conductivity of carbon black-filled immiscible polymer blends by tuning the morphology.* European Polymer Journal, 2016. **78**: p. 106-115.
32. Ren, D., et al., *Effect of the carbon black structure on the stability and efficiency of the conductive network in polyethylene composites.* Journal of Applied Polymer Science, 2013. **129**(6): p. 3382-3389.
33. Spahr, M.E., R. Gilardi, and D. Bonacchi, *Carbon Black for Electrically Conductive Polymer Applications*, in *Encyclopedia of Polymers and Composites*, S. Palsule, Editor. 2021, Springer Berlin Heidelberg: Berlin, Heidelberg. p. 1-20.
34. Wang, M.-J., et al., *Carbon Black*, in *Kirk-Othmer Encyclopedia of Chemical Technology*.
35. Zhang, W., A.A. Dehghani-Sanij, and R.S. Blackburn, *Carbon based conductive polymer composites.* Journal of Materials Science, 2007. **42**(10): p. 3408-3418.
36. Choudhary, N., S. Hwang, and W. Choi, *Carbon Nanomaterials: A Review*, in *Handbook of Nanomaterials Properties*, B. Bhushan, et al., Editors. 2014, Springer Berlin Heidelberg: Berlin, Heidelberg. p. 709-769.
37. Payandehpeyman, J. and M. Mazaheri, *Geometrical and physical effects of nanofillers on percolation and electrical conductivity of polymer carbon-based nanocomposites: a general micro-mechanical model.* Soft Matter, 2023. **19**(3): p. 530-539.
38. Rahaman, M., et al., *Effect of carbons' structure and type on AC electrical properties of polymer composites: predicting the percolation threshold of permittivity through different models.* Colloid and Polymer Science, 2023. **301**(8): p. 1001-1019.
39. Sang, Z., et al., *Dynamic polymer network conductive Nanocomposites: Low percolation threshold and Joule-heating-induced network plasticity.* Chemical Engineering Journal, 2022. **443**: p. 136400.
40. Zambrzycki, M. and A. Fraczek-Szczypta, *Conductive hybrid polymer composites based on recycled carbon fibres and carbon nanofillers.* Journal of Materials Science, 2018. **53**(10): p. 7403-7416.

41. Rybak, A., et al., *Conductive polymer composites based on metallic nanofiller as smart materials for current limiting devices.* Composites Science and Technology, 2010. **70**(2): p. 410-416.
42. Mamunya, Y.P., et al., *Percolation phenomena in polymers containing dispersed iron.* Polymer Engineering & Science, 2002. **42**(1): p. 90-100.
43. Allen, P.B. and W.H. Butler, *Electrical conduction in metals.* Physics Today, 1978. **31**(12): p. 44-49.
44. Sheng, P., E.K. Sichel, and J.I. Gittleman, *Fluctuation-Induced Tunneling Conduction in Carbon-Polyvinylchloride Composites.* Physical Review Letters, 1978. **40**(18): p. 1197-1200.
45. Khan, T., et al., *Insights to low electrical percolation thresholds of carbon-based polypropylene nanocomposites.* Carbon, 2021. **176**: p. 602-631.
46. Genoyer, J., et al., *Graphene and Nanoclay as Processing Aid Agents: A Study on Rheological Behavior in Polystyrene.* C, 2023. **9**(4): p. 96.
47. Moghimian, N. and S. Nazarpour, *The Future of Carbon: An Update on Graphene's Dermal, Inhalation, and Gene Toxicity.* Crystals, 2020. **10**(9): p. 718.
48. Karimi, S., et al., *Photo-stabilization mechanisms of High-Density Polyethylene (HDPE) by a commercial few-layer graphene.* Polymer Engineering & Science, 2023. **63**(11): p. 3879-3890.
49. Karimi, S., et al., *A Review on Graphene's Light Stabilizing Effects for Reduced Photodegradation of Polymers.* Crystals, 2021. **11**(1): p. 3.
50. Sultana, S.M.N., et al., *The Influence of a Commercial Few-Layer Graphene on the Photodegradation Resistance of a Waste Polyolefins Stream and Prime Polyolefin Blends.* Recycling, 2024. **9**(2): p. 29.
51. Diallo, A.K., et al., *Graphene: A multifunctional additive for sustainability.* Sustainable Materials and Technologies, 2022. **33**: p. e00487.
52. Sultana, S.M.N., et al., *Effect of Few-Layer Graphene on the Properties of Mixed Polyolefin Waste Stream.* Crystals, 2023. **13**(2): p. 358.
53. Karásek, L., et al., *Percolation Concept: Polymer-Filler Gel Formation, Electrical Conductivity and Dynamic Electrical Properties of Carbon-Black-Filled Rubbers.* Polymer Journal, 1996. **28**(2): p. 121-126.
54. Helal, E., et al. *Graphene/Thermoplastic Based Composites*. in *2020 IEEE Conference on Electrical Insulation and Dielectric Phenomena (CEIDP)*. 2020.
55. Socher, R., et al., *The influence of matrix viscosity on MWCNT dispersion and electrical properties in different thermoplastic nanocomposites.* Polymer, 2012. **53**(2): p. 495-504.
56. Kou, Y., et al., *Robust networks of interfacial localized graphene in cocontinuous polymer blends.* Journal of Rheology, 2021. **65**(6): p. 1139-1153.
57. Kuester, S., G.M. Barra, and N.R. Demarquette, *Morphology, mechanical properties and electromagnetic shielding effectiveness of poly(styrene-b-ethylene-ran-butylene-b-styrene)/carbon nanotube nanocomposites: effects of maleic anhydride, carbon nanotube loading and processing method.* Polymer International, 2018. **67**(9): p. 1229-1240.
58. Helal, E., et al., *Correlation between morphology, rheological behavior, and electrical behavior of conductive cocontinuous LLDPE/EVA blends containing commercial graphene nanoplatelets.* Journal of Rheology, 2019. **63**(6): p. 961-976.
59. Zhang, C., et al., *Temperature and time dependence of conductive network formation: Dynamic percolation and percolation time.* Polymer, 2006. **47**(1): p. 466-473.
60. Strugova, D., É. David, and N.R. Demarquette, *Linear viscoelasticity of PP/PS/MWCNT composites with co-continuous morphology.* Journal of Rheology, 2022. **66**(4): p. 671-681.
61. Strugova, D., É. David, and N.R. Demarquette, *Effect of steady shear deformation on electrically conductive PP/PS/MWCNT composites.* Journal of Rheology, 2023. **67**(5): p. 977-993.

62. Alig, I., et al., *Filler Networks of Carbon Allotropes of Different Shapes and Dimensions in a Polymer Matrix*, in *Dynamics of Composite Materials*, A. Schönhals and P. Szymoniak, Editors. 2022, Springer International Publishing: Cham. p. 291-333.
63. Pang, H., et al., *Conductive polymer composites with segregated structures.* Progress in Polymer Science, 2014. **39**(11): p. 1908-1933.
64. Vieira, L.d.S., et al., *A review concerning the main factors that interfere in the electrical percolation threshold content of polymeric antistatic packaging with carbon fillers as antistatic agent.* Nano Select, 2022. **3**(2): p. 248-260.
65. Tamjid, E., et al., *Review of sustainable, eco-friendly, and conductive polymer nanocomposites for electronic and thermal applications: current status and future prospects.* Discover Nano, 2024. **19**(1): p. 29.
66. Alig, I., et al., *Establishment, morphology and properties of carbon nanotube networks in polymer melts.* Polymer, 2012. **53**(1): p. 4-28.
67. Münstedt, H. and Z. Starý, *Is electrical percolation in carbon-filled polymers reflected by rheological properties?* Polymer, 2016. **98**: p. 51-60.
68. Xu, S., et al., *The viability and limitations of percolation theory in modeling the electrical behavior of carbon nanotube–polymer composites.* Nanotechnology, 2013. **24**(15): p. 155706.
69. Kirkpatrick, S., *Percolation and Conduction.* Reviews of Modern Physics, 1973. **45**(4): p. 574-588.
70. Balberg, I. and N. Binenbaum, *Computer study of the percolation threshold in a two-dimensional anisotropic system of conducting sticks.* Physical Review B, 1983. **28**(7): p. 3799-3812.
71. Payandehpeyman, J., et al., *Physics-Based Modeling and Experimental Study of Conductivity and Percolation Threshold in Carbon Black Polymer Nanocomposites.* Applied Composite Materials, 2024. **31**(1): p. 127-147.
72. Pötschke, P., et al. *Melt-Mixed PP/MWCNT Composites: Influence of CNT Incorporation Strategy and Matrix Viscosity on Filler Dispersion and Electrical Resistivity*. Polymers, 2019. **11**, DOI: 10.3390/polym11020189.
73. Mutlay, İ. and L.B. Tudoran, *Percolation Behavior of Electrically Conductive Graphene Nanoplatelets/Polymer Nanocomposites: Theory and Experiment.* Fullerenes, Nanotubes and Carbon Nanostructures, 2014. **22**(5): p. 413-433.
74. Wang, G., et al., *Electrical percolation of nanoparticle-polymer composites.* Computational Materials Science, 2018. **150**: p. 102-106.
75. Mao, Z., et al., *Comparison between randomly distributed structure and 3D segregated structure in chlorinated polyethylene/MWCNT composites: electrical conductivity, mechanical property, flame resistance and rheological property.* Composites Science and Technology, 2022. **221**: p. 109338.
76. Kausar, A. and R. Taherian, *3 - Electrical Conductivity Behavior of Polymer Nanocomposite with Carbon Nanofillers*, in *Electrical Conductivity in Polymer-Based Composites*, R. Taherian and A. Kausar, Editors. 2019, William Andrew Publishing. p. 41-72.
77. Tahriri, M., et al., *Graphene and its derivatives: Opportunities and challenges in dentistry.* Materials Science and Engineering: C, 2019. **102**: p. 171-185.
78. Donnet, J.-B.E., *Carbon Black: Science and Technology, Second Edition (2nd ed.)*. 1993: Taylor&Francis.
79. Al-Hartomy, O.A., et al., *Influence of Carbon Black Structure and Specific Surface Area on the Mechanical and Dielectric Properties of Filled Rubber Composites.* International Journal of Polymer Science, 2011. **2011**: p. 521985.
80. Pantea, D., et al., *Electrical conductivity of conductive carbon blacks: influence of surface chemistry and topology.* Applied Surface Science, 2003. **217**(1): p. 181-193.

81. Shen, M.-Y., et al., *Characteristics and Mechanical Properties of Graphene Nanoplatelets-Reinforced Epoxy Nanocomposites: Comparison of Different Dispersal Mechanisms.* Sustainability, 2021. **13**(4): p. 1788.
82. Heidenreich, R.D., W.M. Hess, and L.L. Ban, *A test object and criteria for high resolution electron microscopy.* Journal of Applied Crystallography, 1968. **1**(1): p. 1-19.
83. Xu, J.-Z., et al., *Low-dimensional carbonaceous nanofiller induced polymer crystallization.* Progress in Polymer Science, 2014. **39**(3): p. 555-593.
84. Wang, X., et al., *Comparative Study of Three Carbon Additives: Carbon Nanotubes, Graphene, and Fullerene-C60, for Synthesizing Enhanced Polymer Nanocomposites.* Nanomaterials, 2020. **10**(5): p. 838.
85. Wang, Y. and G.J. Weng, *Electrical Conductivity of Carbon Nanotube- and Graphene-Based Nanocomposites*, in *Micromechanics and Nanomechanics of Composite Solids*, S.A. Meguid and G.J. Weng, Editors. 2018, Springer International Publishing: Cham. p. 123-156.
86. Torrisi, L., et al., *Measurements on Five Characterizing Properties of Graphene Oxide and Reduced Graphene Oxide Foils.* physica status solidi (a), 2022. **219**(6): p. 2100628.
87. Iijima, S. and T. Ichihashi, *Single-shell carbon nanotubes of 1-nm diameter.* Nature, 1993. **363**(6430): p. 603-605.
88. Wang, X.-Y., A. Narita, and K. Müllen, *Precision synthesis versus bulk-scale fabrication of graphenes.* Nature Reviews Chemistry, 2017. **2**(1): p. 0100.
89. Jiménez-Suárez, A. and S.G. Prolongo, *Graphene Nanoplatelets.* Applied Sciences, 2020. **10**(5): p. 1753.
90. Gavallas, P., D. Savvas, and G. Stefanou, *Mechanical properties of graphene nanoplatelets containing random structural defects.* Mechanics of Materials, 2023. **180**: p. 104611.
91. Urade, A.R., I. Lahiri, and K.S. Suresh, *Graphene Properties, Synthesis and Applications: A Review.* JOM, 2023. **75**(3): p. 614-630.
92. Marsden, A.J., et al., *Electrical percolation in graphene–polymer composites.* 2D Materials, 2018. **5**(3): p. 032003.
93. Strugova, D., et al. *Ultra-Low Percolation Threshold Induced by Thermal Treatments in Co-Continuous Blend-Based PP/PS/MWCNTs Nanocomposites*. Nanomaterials, 2021. **11**, DOI: 10.3390/nano11061620.
94. Bauhofer, W. and J.Z. Kovacs, *A review and analysis of electrical percolation in carbon nanotube polymer composites.* Composites Science and Technology, 2009. **69**(10): p. 1486-1498.
95. Choi, H.-J., et al., *Electrical percolation threshold of carbon black in a polymer matrix and its application to antistatic fibre.* Scientific Reports, 2019. **9**(1): p. 6338.
96. Wang, P., et al., *Ultralow electrical percolation in melt-compounded polymer composites based on chemically expanded graphite.* Composites Science and Technology, 2018. **158**: p. 147-155.
97. Quintanilla, J., *Measurement of the percolation threshold for fully penetrable disks of different radii.* Physical Review E, 2001. **63**(6): p. 061108.
98. Tarani, E., et al., *Influence of Graphene Platelet Aspect Ratio on the Mechanical Properties of HDPE Nanocomposites: Microscopic Observation and Micromechanical Modeling.* Polymers, 2020. **12**(8): p. 1719.
99. Li, J. and S.-L. Zhang, *Finite-size scaling in stick percolation.* Physical Review E, 2009. **80**(4): p. 040104.
100. Ghislandi, M., et al., *Electrical conductivities of carbon powder nanofillers and their latex-based polymer composites.* Composites Part A: Applied Science and Manufacturing, 2013. **53**: p. 145-151.
101. Pan, Y. and L. Li, *Percolation and gel-like behavior of multiwalled carbon nanotube/polypropylene composites influenced by nanotube aspect ratio.* Polymer, 2013. **54**(3): p. 1218-1226.

102. Rahaman, M., et al., *4 - Electrical conductivity of polymer-graphene composites*, in *Polymer Nanocomposites Containing Graphene*, M. Rahaman, et al., Editors. 2022, Woodhead Publishing. p. 107-139.
103. Al-Saleh, M.H., *Influence of polymer structure on the electrical resistivity of nanocomposite materials.* Synthetic Metals, 2020. **265**: p. 116409.
104. Castro Martínez, M., S. Hernández López, and E. Vigueras Santiago, *Relationship between Polymer Dielectric Constant and Percolation Threshold in Conductive Poly(styrene)-Type Polymer and Carbon Black Composites.* Journal of Nanomaterials, 2015. **2015**: p. 607896.
105. Kuan, C.-F., et al., *Mechanical and electrical properties of multi-wall carbon nanotube/poly(lactic acid) composites.* Journal of Physics and Chemistry of Solids, 2008. **69**(5): p. 1395-1398.
106. Sullivan, E.M., et al., *Understanding the effect of polymer crystallinity on the electrical conductivity of exfoliated graphite nanoplatelet/polylactic acid composite films.* Journal of Polymer Research, 2014. **21**(10): p. 563.
107. Bilotti, E., et al., *Controlling the dynamic percolation of carbon nanotube based conductive polymer composites by addition of secondary nanofillers: The effect on electrical conductivity and tuneable sensing behaviour.* Composites Science and Technology, 2013. **74**: p. 85-90.
108. Combessis, A., et al., *Understanding dynamic percolation mechanisms in carbonaceous polymer nanocomposites through impedance spectroscopy: Experiments and modeling.* Journal of Applied Physics, 2014. **116**(3).
109. Tjong, S.C., G.D. Liang, and S.P. Bao, *Electrical behavior of polypropylene/multiwalled carbon nanotube nanocomposites with low percolation threshold.* Scripta Materialia, 2007. **57**(6): p. 461-464.
110. Naji, A., P. Pötschke, and A. Ameli. *Electrical Conductivity of Multifunctional Blend Composites of Polycarbonate and Polyethylene With Hybrid Fillers*. in *ASME 2022 Conference on Smart Materials, Adaptive Structures and Intelligent Systems*. 2022.
111. Qi, X.-d., et al., *Selective localization of carbon nanotubes and its effect on the structure and properties of polymer blends.* Progress in Polymer Science, 2021. **123**: p. 101471.
112. Liebscher, M., et al., *Dispersion of graphite nanoplates in melt mixed PC/SAN polymer blends and its influence on rheological and electrical properties.* Polymer, 2020. **200**: p. 122577.
113. Sultana, S.M.N., et al., *Tailoring MWCNT Dispersion, Blend Morphology and EMI Shielding Properties by Sequential Mixing Strategy in Immiscible PS/PVDF Blends.* Journal of Electronic Materials, 2020. **49**(3): p. 1588-1600.
114. Kurusu, R.S., et al., *The Role of Selectively Located Commercial Graphene Nanoplatelets in the Electrical Properties, Morphology, and Stability of EVA/LLDPE Blends.* Macromolecular Materials and Engineering, 2018. **303**(9): p. 1800187.
115. Bai, L., et al., *Localizing graphene at the interface of cocontinuous polymer blends: Morphology, rheology, and conductivity of cocontinuous conductive polymer composites.* Journal of Rheology, 2017. **61**(4): p. 575-587.
116. Thongruang, W., R.J. Spontak, and C.M. Balik, *Bridged double percolation in conductive polymer composites: an electrical conductivity, morphology and mechanical property study.* Polymer, 2002. **43**(13): p. 3717-3725.
117. Maiti, S., et al., *Polystyrene/MWCNT/Graphite Nanoplate Nanocomposites: Efficient Electromagnetic Interference Shielding Material through Graphite Nanoplate–MWCNT–Graphite Nanoplate Networking.* ACS Applied Materials & Interfaces, 2013. **5**(11): p. 4712-4724.
118. Salehiyan, R. and S.S. Ray, *Tuning the Conductivity of Nanocomposites through Nanoparticle Migration and Interface Crossing in Immiscible Polymer Blends: A Review on Fundamental Understanding.* Macromolecular Materials and Engineering, 2019. **304**(2): p. 1800431.

119. Nofar, M., R. Salehiyan, and S.S. Ray, *Influence of nanoparticles and their selective localization on the structure and properties of polylactide-based blend nanocomposites.* Composites Part B: Engineering, 2021. **215**: p. 108845.
120. Valera, T.S., A.T. Morita, and N.R. Demarquette, *Study of Morphologies of PMMA/PP/PS Ternary Blends.* Macromolecules, 2006. **39**(7): p. 2663-2675.
121. Sumita, M., et al., *Dispersion of fillers and the electrical conductivity of polymer blends filled with carbon black.* Polymer Bulletin, 1991. **25**(2): p. 265-271.
122. Demarquette, N.R., *Evaluation of experimental techniques for determining interfacial tension between molten polymers.* International Materials Reviews, 2003. **48**(4): p. 247-269.
123. Göldel, A., et al., *The kinetics of CNT transfer between immiscible blend phases during melt mixing.* Polymer, 2012. **53**(2): p. 411-421.
124. Taguet, A., P. Cassagnau, and J.M. Lopez-Cuesta, *Structuration, selective dispersion and compatibilizing effect of (nano)fillers in polymer blends.* Progress in Polymer Science, 2014. **39**(8): p. 1526-1563.
125. Wang, J., et al., *Enhancing the electrical conductivity of PP/CNT nanocomposites through crystal-induced volume exclusion effect with a slow cooling rate.* Composites Part B: Engineering, 2020. **183**: p. 107663.
126. Kazemi, Y., et al., *Conductive network formation and destruction in polypropylene/carbon nanotube composites via crystal control using supercritical carbon dioxide.* Polymer, 2017. **129**: p. 179-188.
127. Jia, L.-C., et al., *Electrically conductive and electromagnetic interference shielding of polyethylene composites with devisable carbon nanotube networks.* Journal of Materials Chemistry C, 2015. **3**(36): p. 9369-9378.
128. Nicole R. Demarquette, D.J.C., in *Nanocomposite Materials Synthesis, Properties and Applications*, J. Parameswaranpillai, Hameed, N., Kurian, T., & Yu, Y. (Eds.). Editor. 2016, Taylor&Francis. p. 32.
129. Ren, J. and R. Krishnamoorti, *Nonlinear Viscoelastic Properties of Layered-Silicate-Based Intercalated Nanocomposites.* Macromolecules, 2003. **36**(12): p. 4443-4451.
130. Du, F., et al., *Nanotube Networks in Polymer Nanocomposites: Rheology and Electrical Conductivity.* Macromolecules, 2004. **37**(24): p. 9048-9055.
131. Sun, X.-R., et al., *Effect of phase coarsening under melt annealing on the electrical performance of polymer composites with a double percolation structure.* Physical Chemistry Chemical Physics, 2018. **20**(1): p. 137-147.
132. Zhang, C., et al., *Electric field controlled formation and dissociation of multiwalled carbon nanotube conductive pathways in a polymer melt.* Applied Physics Letters, 2009. **94**(11).
133. Yu, W., W. Zhou, and C. Zhou, *Linear viscoelasticity of polymer blends with co-continuous morphology.* Polymer, 2010. **51**(9): p. 2091-2098.
134. Göldel, A., et al., *Shape-Dependent Localization of Carbon Nanotubes and Carbon Black in an Immiscible Polymer Blend during Melt Mixing.* Macromolecules, 2011. **44**(15): p. 6094-6102.
135. Schyns, Z.O.G. and M.P. Shaver, *Mechanical Recycling of Packaging Plastics: A Review.* Macromolecular Rapid Communications, 2021. **42**(3): p. 2000415.
136. da Silva, D.J. and H. Wiebeck, *Current options for characterizing, sorting, and recycling polymeric waste.* Progress in Rubber, Plastics and Recycling Technology, 2020. **36**(4): p. 284-303.
137. Jagadeesh, P., et al., *Sustainable recycling technologies for thermoplastic polymers and their composites: A review of the state of the art.* Polymer Composites, 2022. **43**(9): p. 5831-5862.
138. Schweighuber, A., et al., *Investigations on the influence of multiple extrusion on the degradation of polyolefins.* Polymer Degradation and Stability, 2021. **192**: p. 109689.

139. Jubinville, D., et al., *Thermo-mechanical recycling of polypropylene for the facile and scalable fabrication of highly loaded wood plastic composites.* Composites Part B: Engineering, 2021. **219**: p. 108873.
140. Pegoretti, A., *Recycling concepts for short-fiber-reinforced and particle-filled thermoplastic composites: A review.* Advanced Industrial and Engineering Polymer Research, 2021. **4**(2): p. 93-104.
141. Archibong, F.N., et al., *An overview on the recycling of waste ground tyre rubbers in thermoplastic matrices: Effect of added fillers.* Resources, Conservation and Recycling, 2021. **175**: p. 105894.
142. Montagna, L.S., et al., *A viable strategy to recycle post-used carbon fiber thermoset composites as a multi-functional filler for PP composites.* Journal of Thermoplastic Composite Materials, 2024. **37**(2): p. 445-465.
143. Dong, F., et al., *A tough, healable, and recyclable conductive polyurethane/carbon nanotube composite.* Journal of Colloid and Interface Science, 2023. **631**: p. 239-248.
144. Yan, Q., M. Zhou, and H. Fu, *A reversible and highly conductive adhesive: towards self-healing and recyclable flexible electronics.* Journal of Materials Chemistry C, 2020. **8**(23): p. 7772-7785.
145. Stan, F., et al., *Mechanical Recycling of Low-Density Polyethylene/Carbon Nanotube Composites and Its Effect on Material Properties.* Journal of Manufacturing Science and Engineering, 2019. **141**(9).
146. Rahaman, M., et al., *Recycling and Reusing Polyethylene Waste as Antistatic and Electromagnetic Interference Shielding Materials.* International Journal of Polymer Science, 2020. **2020**: p. 6421470.
147. Tong, D.J.Y., et al., *Conductive Polymer Composites Made from Polypropylene and Recycled Graphite Scrap.* Journal of Physical Science, 2021.
148. Jena, K.K., A. AlFantazi, and A.T. Mayyas, *Efficient and cost-effective hybrid composite materials based on thermoplastic polymer and recycled graphite.* Chemical Engineering Journal, 2022. **430**: p. 132667.
149. Di Persio, F., et al., *Recyclability of novel energy harvesting and storage technologies for IoT and wireless sensor networks.* Journal of Cleaner Production, 2024. **435**: p. 140525.
150. Carroccio, S.C., et al., *Impact of nanoparticles on the environmental sustainability of polymer nanocomposites based on bioplastics or recycled plastics – A review of life-cycle assessment studies.* Journal of Cleaner Production, 2022. **335**: p. 130322.
151. Alrefaee, S.H., et al., *Recycled polystyrene/polyvinylpyrrolidone/reduced graphene oxide nanocomposites for optoelectronic devices.* Journal of Materials Research and Technology, 2023. **25**: p. 2631-2640.
152. Velásquez, E., et al., *Developing Post-Consumer Recycled Flexible Polypropylene and Fumed Silica-Based Nanocomposites with Improved Processability and Thermal Stability.* Polymers, 2023. **15**(5): p. 1142.
153. Zdiri, K., et al., *Reinforcement of recycled PP polymers by nanoparticles incorporation.* Green Chemistry Letters and Reviews, 2018. **11**(3): p. 296-311.
154. Zare, Y., *Recent progress on preparation and properties of nanocomposites from recycled polymers: A review.* Waste Management, 2013. **33**(3): p. 598-604.
155. López de Dicastillo, C., et al., *The use of nanoadditives within recycled polymers for food packaging: Properties, recyclability, and safety.* Comprehensive Reviews in Food Science and Food Safety, 2020. **19**(4): p. 1760-1776.
156. Marotta, A., et al., *Tuning the Morphology of HDPE/PP/PET Ternary Blends by Nanoparticles: A Simple Way to Improve the Performance of Mixed Recycled Plastics.* Polymers, 2022. **14**(24): p. 5390.

157. Ferreira, E.H.C., R.J.E. Andrade, and G.J.M. Fechine, *The "Superlubricity State" of Carbonaceous Fillers on Polyethylene-Based Composites in a Molten State.* Macromolecules, 2019. **52**(24): p. 9620-9631.
158. Liu, M. and A.R. Horrocks, *Effect of Carbon Black on UV stability of LLDPE films under artificial weathering conditions.* Polymer Degradation and Stability, 2002. **75**(3): p. 485-499.
159. Horrocks, A.R. and M. Liu, *UV stabilising synergies between carbon black and hindered light stabilisers in linear low density polyethylene films.* Macromolecular Symposia, 2003. **202**(1): p. 199-220.
160. Shimizu, T., et al., *Radical scavenging activity of carbon nanotubes: toward appropriate selection of a radical initiator.* RSC Advances, 2020. **10**(49): p. 29419-29423.
161. Dorigato, A. and G. Fredi, *Effect of nanofillers addition on the compatibilization of polymer blends.* Advanced Industrial and Engineering Polymer Research, 2023.
162. Shah, R.S., S. Bryant, and M. Trifkovic, *Particle-size dependent stability of co-continuous polymer blends.* Journal of Rheology, 2023. **67**(4): p. 863-863.
163. Shah, R.S., S. Bryant, and M. Trifkovic, *Decoupling the interplay of polymer properties and particle size in stability of co-continuous blend composites.* Physics of Fluids, 2023. **35**(5).
164. Maris, J., et al., *Mechanical recycling: Compatibilization of mixed thermoplastic wastes.* Polymer Degradation and Stability, 2018. **147**: p. 245-266.
165. Seyedi, M., et al., *Toward Mechanical Recycling of Polystyrene/Polypropylene Blends with Bottlebrush-Modified Graphene Oxide as a Compatibilizer.* ACS Applied Materials & Interfaces, 2022. **14**(30): p. 35074-35086.
166. Ajitha, A.R., L.P. Mathew, and S. Thomas, *Chapter 6 - Compatibilization of polymer blends by micro and nanofillers*, in *Compatibilization of Polymer Blends*, A. A.R and S. Thomas, Editors. 2020, Elsevier. p. 179-203.
167. Cao, Y., et al., *Compatibilization of Immiscible Polymer Blends Using Graphene Oxide Sheets.* ACS Nano, 2011. **5**(7): p. 5920-5927.
168. Genoyer, J., et al., *Compatibilization mechanism induced by organoclay in PMMA/PS blends.* Journal of Rheology, 2017. **61**(4): p. 613-626.
169. Genoyer, J., N.R. Demarquette, and J. Soulestin, *Effect of clay particles size and location on coalescence in PMMA/PS blends.* Journal of Rheology, 2019. **63**(6): p. 883-893.
170. Altobelli, R., M. Salzano de Luna, and G. Filippone, *Interfacial crowding of nanoplatelets in co-continuous polymer blends: assembly, elasticity and structure of the interfacial nanoparticle network.* Soft Matter, 2017. **13**(37): p. 6465-6473.
171. Gegenhuber, T., et al., *"Patchy" Carbon Nanotubes as Efficient Compatibilizers for Polymer Blends.* ACS Macro Letters, 2016. **5**(3): p. 306-310.
172. Wang, B., et al., *Reactive graphene as highly efficient compatibilizer for cocontinuous poly(lactic acid)/poly(ε-caprolactone) blends toward robust biodegradable nanocomposites.* Composites Science and Technology, 2022. **221**: p. 109326.
173. Yang, X., et al., *High-reactive silica nanosheets as compatibilizers for immiscible PLLA/PBAT polymer blends.* Composites Science and Technology, 2023. **236**: p. 109979.
174. Walther, A., K. Matussek, and A.H.E. Müller, *Engineering Nanostructured Polymer Blends with Controlled Nanoparticle Location using Janus Particles.* ACS Nano, 2008. **2**(6): p. 1167-1178.
175. Kuila, T., et al., *Chemical functionalization of graphene and its applications.* Progress in Materials Science, 2012. **57**(7): p. 1061-1105.
176. Shanmugam, V., et al., *Polymer Recycling in Additive Manufacturing: an Opportunity for the Circular Economy.* Materials Circular Economy, 2020. **2**(1): p. 11.
177. Zander, N.E., et al., *Recycled polypropylene blends as novel 3D printing materials.* Additive Manufacturing, 2019. **25**: p. 122-130.

178. Santander, P., et al., *Closed loop supply chain network for local and distributed plastic recycling for 3D printing: a MILP-based optimization approach.* Resources, Conservation and Recycling, 2020. **154**: p. 104531.
179. *Additive Manufacturing for Plastic Recycling*

Efforts in Boosting A Circular Economy. 2022: CRC Press.
180. Gomes, T.E.P., et al., *Controlling the properties of parts 3D printed from recycled thermoplastics: A review of current practices.* Polymer Degradation and Stability, 2022. **196**: p. 109850.
181. Vidakis, N., et al., *Sustainable Additive Manufacturing: Mechanical Response of Polypropylene over Multiple Recycling Processes.* Sustainability, 2021. **13**(1): p. 159.
182. Goh, G.D., et al., *Large-format additive manufacturing of polymers: a review of fabrication processes, materials, and design.* Virtual and Physical Prototyping, 2024. **19**(1): p. e2336160.
183. Hidalgo-Carvajal, D., et al., *Recycled PLA for 3D Printing: A Comparison of Recycled PLA Filaments from Waste of Different Origins after Repeated Cycles of Extrusion.* Polymers, 2023. **15**(17): p. 3651.
184. Vidakis, N., et al., *Sustainable Additive Manufacturing: Mechanical Response of Acrylonitrile-Butadiene-Styrene over Multiple Recycling Processes.* Sustainability, 2020. **12**(9): p. 3568.
185. Yan, Y., et al., *Progress and opportunities in additive manufacturing of electrically conductive polymer composites.* Materials Today Advances, 2023. **17**: p. 100333.
186. Ryan, K.R., et al., *Additive manufacturing (3D printing) of electrically conductive polymers and polymer nanocomposites and their applications.* eScience, 2022. **2**(4): p. 365-381.
187. Hohimer, C.J., et al., *3D printed conductive thermoplastic polyurethane/carbon nanotube composites for capacitive and piezoresistive sensing in soft pneumatic actuators.* Additive Manufacturing, 2020. **34**: p. 101281.
188. Mudhar, R., et al., *Electrical and Magnetic Properties of 3D Printed Integrated Conductive Biodegradable Polymer Nanocomposites for Sustainable Electronics Development.* Journal of Composites Science, 2022. **6**(11): p. 345.
189. Kwok, S.W., et al., *Electrically conductive filament for 3D-printed circuits and sensors.* Applied Materials Today, 2017. **9**: p. 167-175.
190. Dawoud, M., I. Taha, and S.J. Ebeid, *Strain sensing behaviour of 3D printed carbon black filled ABS.* Journal of Manufacturing Processes, 2018. **35**: p. 337-342.
191. Mora, A., P. Verma, and S. Kumar, *Electrical conductivity of CNT/polymer composites: 3D printing, measurements and modeling.* Composites Part B: Engineering, 2020. **183**: p. 107600.
192. Gnanasekaran, K., et al., *3D printing of CNT- and graphene-based conductive polymer nanocomposites by fused deposition modeling.* Applied Materials Today, 2017. **9**: p. 21-28.